Properties of Tri- and Tetracarboxylate Ca^{2+} Indicators in Frog Skeletal Muscle Fibers

Mingdi Zhao, S. Hollingworth, and S. M. Baylor
Department of Physiology, University of Pennsylvania School of Medicine, Philadelphia, Pennsylvania 19104-6085 USA

ABSTRACT Recently a number of lower-affinity fluorescent Ca^{2+} indicators have become available with principal absorbance bands at visible wavelengths. This article evaluates these indicators, as well as two shorter wavelength indicators, mag-fura-5 and mag-indo-1, for their suitability as rapid Ca^{2+} indicators in frog skeletal muscle fibers. With three lower-affinity tricarboxylate indicators (mag-fura-5, mag-indo-1, and magnesium orange), the change in fluorescence in response to an action potential (ΔF) appeared to track the myoplasmic Ca^{2+} transient ($\Delta[Ca^{2+}]$) without delay. With three lower-affinity tetracarboxylate indicators (BTC, calcium-orange-5N, and calcium-green-5N) and one tricarboxylate indicator (magnesium green), ΔF responded to $\Delta[Ca^{2+}]$ with a small delay. Unfortunately, with the tetracarboxylate indicators, other problems were detected that appear to limit their usefulness as reliable Ca^{2+} indicators. Surprisingly, ΔF from mag-fura-red, another tricarboxylate indicator, was biphasic (with 480 nm excitation), a feature that also greatly limits its usefulness. With several of the indicators, estimates were obtained for the myoplasmic value of $K_{D,\,Ca}$ (the indicator's dissociation constant for Ca^{2+}) and found to be elevated severalfold in comparison with the value measured in a simple salt solution. These and other problems related to the quantitative use of Ca^{2+} indicators in the intracellular environment are evaluated and discussed.

INTRODUCTION

A common goal of studies from a number of laboratories has been to use Ca^{2+} indicator dyes to measure the change in intracellular free calcium concentration ($\Delta[Ca^{2+}]$) that accompanies activation in many cell types. In studies with twitch muscle fibers, the achievement of this goal has been complicated by a number of technical problems related to the binding of indicator molecules to intracellular constituents (Beeler et al., 1980; Baylor et al., 1982a, 1986; Maylie et al., 1987a,b,c; Baylor and Hollingworth, 1988).

Some of these problems are illustrated by higher-affinity fluorescent indicators of the tetracarboxylate family (Tsien, 1980), including fura-2 (Grynkiewicz et al., 1985), fura-red (DeMarinis et al., 1990), and fluo-3 (Minta et al., 1989). In a simple salt solution, these indicators react with Ca^{2+} with 1:1 stoichiometry, with values of $K_{D,\,Ca}$ (the indicator's apparent dissociation constant for Ca^{2+}) of 0.2–0.5 μM. However, other in vitro measurements show that these indicators readily bind to cell constituents, such as soluble proteins, and that protein binding alters a number of indicator properties that are important for accurate quantification of $[Ca^{2+}]$ (Konishi et al., 1988; Uto et al., 1991; Hove-Madsen and Bers, 1992; Kurebayashi et al., 1993; Harkins et al., 1993; Baker et al., 1994; Bassani et al., 1995). These include the indicator's absorbance and fluorescence spectra, its fluorescence intensity, and the value of $K_{D,\,Ca}$. For example, with fura-2, fura-red, and fluo-3, protein binding increases $K_{D,\,Ca}$ by two- to fourfold over the values measured in a simple salt solution, an effect that implies some alteration of the forward (k_{+1}) and/or backward (k_{-1}) rate constants that control the reaction between indicator and Ca^{2+}.

When introduced into frog single muscle fibers, fura-2, fura-red, and fluo-3 also appear to bind to cell constituents, and the percentage of bound indicator is estimated to be large (70–90%) (Baylor and Hollingworth, 1988; Konishi et al., 1988; Kurebayashi et al., 1993; Harkins et al., 1993). In myoplasm, the properties of bound indicator appear to be altered in ways similar to those detected for protein-bound indicator in vitro. Furthermore, kinetic experiments indicate that the effective values of k_{+1} and k_{-1} in myoplasm (Baylor and Hollingworth, 1988; Klein et al., 1988; Kurebayashi et al., 1993; Harkins et al., 1993; Pape et al., 1993) are substantially smaller than the corresponding values measured in a simple salt solution (Kao and Tsien, 1988; Lattanzio and Bartschat, 1991). The reductions in k_{+1} are probably severalfold greater than apply to k_{-1}, with the result that the myoplasmic values of $K_{D,\,Ca}$ are increased severalfold. However, the exact values of the rate constants in myoplasm and of $K_{D,\,Ca}$, are uncertain. Hence estimates obtained with these indicators for the resting level of $[Ca^{2+}]$ and the amplitude and time course of $\Delta[Ca^{2+}]$ in response to an action potential are uncertain.

In contrast, results obtained in frog twitch muscle fibers with two lower-affinity indicators can be interpreted more confidently. These indicators, which also react with Ca^{2+} with 1:1 stoichiometry, are i) purpurate-3,3′diacetic acid (PDAA; in vitro $K_{D,\,Ca}$ = 950 μM), an absorbance indicator related to murexide (Hirota et al., 1989), and ii) furaptra (in vitro $K_{D,\,Ca}$ = 44 μM), a fluorescent indicator with a fluorophore identical to that of fura-2 but with a tricarboxylate rather than a tetracarboxylate Ca^{2+}-binding pocket (Raju et al., 1990). (*Note:* furaptra, because of its reduced

Received for publication 1 September 1995 and in final form 7 November 1995.

Address reprint requests to Dr. S. M. Baylor, Department of Physiology, University of Pennsylvania School of Medicine, Philadelphia, PA 19104-6085. Fax: 215-573-5851; E-mail: baylor@a1.mscf.upenn.edu.

0006-3495/96/02/896/21 $2.00

selectivity for Ca^{2+} over Mg^{2+}, is sold commercially under the name "mag-fura-2.")

In intact frog fibers, both PDAA and furaptra appear to bind less heavily to myoplasmic constituents than do the higher-affinity tetracarboxylate indicators; the estimated bound percentages are 24–42% for PDAA and 42–51% for furaptra (Konishi and Baylor, 1991; Konishi et al., 1991; see also Hirota et al., 1989). Interestingly, both indicators appear to report the correct time course of $\Delta[Ca^{2+}]$ (Hirota et al., 1989; Baylor et al., 1989; Konishi and Baylor, 1991; Konishi et al., 1991). This situation likely arises because the in vitro values of k_{-1} are sufficiently large for both indicators that, even with some reduction associated with indicator binding in vivo, the rates remain large enough that the optical signals from PDAA and furaptra track $\Delta[Ca^{2+}]$ without delay. Some discrepancy exists, however, in the calibration of the amplitude of $\Delta[Ca^{2+}]$. If the calibration is based on constants measured in a simple salt solution, the average amplitude of $\Delta[Ca^{2+}]$ estimated with furaptra is about half that estimated with PDAA. Because the binding of indicator to intracellular constituents appears to be somewhat less for PDAA, the amplitude of $\Delta[Ca^{2+}]$ is considered to be more reliable when estimated with PDAA than with furaptra (Konishi et al., 1991). On the other hand, furaptra has the advantage of responding to Ca^{2+} with a change in fluorescence (as well as absorbance); in muscle, fluorescence signals have a reduced susceptibility to movement artifacts and little or no interference from intrinsic optical signals.

Recently other lower-affinity fluorescent indicators have become available that may also report accurate information about the time course and, possibly, the amplitude of $\Delta[Ca^{2+}]$. Some of these indicators offer potential advantages over furaptra, including a) the selectivity for Ca^{2+} over Mg^{2+} expected of a tetracarboxylate compound (Tsien, 1980), which should minimize interference in the Ca^{2+}-related signals from concurrent changes in intra-cellular free $[Mg^{2+}]$ ($\Delta[Mg^{2+}]$), and b) absorbance bands centered at visible wavelengths, which should permit a more thorough study of indicator properties in the intracellular environment. For example, in larger cells such as skeletal muscle fibers, visible absorbance bands allow the possibility of accurate measurements of indicator-related absorbance at rest and during activity; this information complements in important ways the information available from fluorescence measurements alone (Baylor and Hollingworth, 1988; Kurebayashi et al., 1993; Harkins et al., 1993).

The experiments described in this article were undertaken to assess the kinetic, spectral, and selectivity properties of these newer lower-affinity fluorescent indicators, and hence their potential value for studies of $\Delta[Ca^{2+}]$ in skeletal muscle and other cells. It was also hoped that, by use of similar techniques to examine a number of indicators in parallel, some general patterns of indicator properties might emerge. For comparative purposes, signals from five higher-affinity fluorescent indicators (calcium-green-1, calcium-green-2, calcium-orange, indo-1, and quin-2) were also measured. Of the eight lower-affinity indicators examined, six have major absorbance bands at visible wavelengths. Of these, calcium-orange-5N, calcium-green-5N, and BTC are tetracarboxylate compounds, whereas magnesium orange, magnesium green, and mag-fura-red are tricarboxylate compounds. The other two lower-affinity indicators studied (mag-fura-5 and mag-indo-1) are tricarboxylate compounds with absorbance bands at shorter wavelength ($\lambda < 420$ nm) and are closely related to furaptra.

MATERIALS AND METHODS

The experimental methods were similar to those previously described (Baylor and Hollingworth, 1988; Konishi et al., 1991; Kurebayashi et al., 1993; Harkins et al., 1993). All indicators were purchased from Molecular Probes (Eugene, OR) in their permanently charged form (usually tri-, tetra-, or penta-K^+ forms).

In vitro measurements

In this article, the relative affinity of a Ca^{2+} indicator is defined with respect to the indicator's dissociation constant for Ca^{2+} ($K_{D,\,Ca}$) as measured in a salt solution of ionic strength 0.1–0.15 M and at a temperature of 16–22°C. The term "higher affinity" is used if $K_{D,\,Ca} \leq 0.6$ μM and "lower affinity" if $K_{D,\,Ca}$ is ≥ 6 μM. Column 3 of Table 1 lists in vitro values of $K_{D,\,Ca}$ of the five higher-affinity and nine lower-affinity indicators studied. For the six tricarboxylate indicators, column 4 of Table 1 lists in vitro values of $K_{D,\,Mg}$ (the indicator's dissociation constant for Mg^{2+}). Column 5 of Table 1 gives the ratio of the two K_D values. The tricarboxylate indicators have a reduced selectivity for Ca^{2+} over Mg^{2+} (Raju et al., 1990), and in muscle fibers, their fluorescence signals at later times after stimulation appear to reflect a significant contribution from $\Delta[Mg^{2+}]$ (Konishi et al., 1991; Konishi et al., 1993). In contrast, for the tetracarboxylate indicators, $K_{D,\,Mg}/K_{D,\,Ca}$ is generally greater than 10^4 (e.g., Grynkiewicz et al., 1985), and any Mg^{2+} interference in the intracellular Ca^{2+} signal is expected to be negligible.

The K_D values listed in Table 1 were either taken from the literature or estimated from in vitro titrations in standard buffer solutions by an absorbance method similar to that previously described for furaptra (Konishi et al., 1991). These titrations utilized the wavelength ranges given in column 6 of Table 1. With some of the indicators, the Ca^{2+}- and/or Mg^{2+}-related absorbance changes were relatively small; nevertheless, the data were sufficiently well resolved that, when least-squares fitted by the 1:1 binding equation, they yielded an apparently well-determined value of K_D.

In vivo measurements

An intact single fiber, dissected from the semi-tendinosus or iliofibularis muscle of *Rana temporaria*, was mounted on a horizontal optical bench apparatus in a temperature-controlled chamber with quartz windows. The normal Ringer's solution bathing the fiber contained (in mM): 120 NaCl, 2.5 KCl, 1.8 $CaCl_2$ and 5 PIPES (piperazine-*N,N'*-bis[2-ethane-sulfonic acid]) (pH 7.1, 16°C). To minimize movement artifacts in the optical traces, the fiber was stretched to a long sarcomere length (3.6–4.3 μm) and lowered over a pair of supporting pedestals, which were separated by ~1 cm. An indicator, dissolved in distilled water at a concentration of 10–30 mM, was pressure injected into the fiber from a micropipette filled with the indicator.

Fiber optical measurements were based primarily on fluorescence rather than absorbance. Fluorescence recordings were made from a 300-μm length of fiber usually centered at the injection site. Although the concentration of indicator in myoplasm ($[D_T]$) was not routinely measured, $[D_T]$

TABLE 1 In vitro values of $K_{D,Ca}$ and $K_{D,Mg}$

Indicator (1)	Molecular weight (2)	$K_{D,Ca}$ (μM) (3)	$K_{D,Mg}$ (mM) (4)	$\frac{K_{D,Mg}}{K_{D,Ca}}$ (5)	Titration wavelengths (nm) (6)
A. Higher-affinity Ca^{2+} indicators					
Calcium-green-1	913	0.19*	—	—	—
Calcium-green-2	1354	0.57*	—	—	—
Calcium orange	931	0.33*	—	—	—
Indo-1	645	0.25*	—	—	—
Quin-2	542	0.13*	—	—	—
B. Lower-affinity tetracarboxylate Ca^{2+} indicators					
BTC	688	26	—	—	350–550
Calcium-green-5N	958	63, 85‡	—	—	400–600
Calcium-orange-5N	976	55, 53§	—	—	300–500
C. Lower-affinity tricarboxylate Ca^{2+} indicators					
Furaptra	431	44¶	5.3¶	120	300–500
Magnesium green	721	7	2.4	343	300–450
Magnesium orange	739	43	8.2	191	300–420
Mag-fura-5	445	31	4.3	139	300–500
Mag-fura-red	447	55	9.3	169	380–660
Mag-indo-1	438	29	7.6	262	300–460

Columns 1 and 2 list the indicators and the molecular weights of their anionic form. Columns 3 and 4 give the indicators' dissociation constants for Ca^{2+} ($K_{D,Ca}$) and Mg^{2+} ($K_{D,Mg}$), as determined in an vitro salt solution (e.g., 0.1 M KCl) at 16–22°C, an ionic strength of 0.1–0.15 M, and a pH of 7.0–7.1. K_D values were either taken from the literature (*Haugland, 1992; ‡Vergara and Escobar, 1993; §Cifuentes et al., 1993; ¶Konishi et al., 1991) or determined in our own in vitro absorbance titrations at the wavelengths given in column 6. $K_{D,Ca}$ was determined in the absence of Mg^{2+} and $K_{D,Mg}$ in the absence of Ca^{2+}. $K_{D,Mg}$ was not measured for the tetracarboxylate indicators (dash in column 4), because they have generally high selectivity for Ca^{2+} over Mg^{2+} ($K_{D,Mg}/K_{D,Ca} > 10^4$). For the tricarboxylates indicators, $K_{D,Mg}/K_{D,Ca}$ is given in column 5.

at the recording site was, in general, sufficiently small that $\Delta[Ca^{2+}]$ was not perturbed significantly by the calcium buffer capacity or possible pharmacological actions of the indicator. This conclusion is supported by checks that i) the amplitude of the fiber's intrinsic birefringence signal ("second component"; Baylor and Oetliker, 1977) was not changed significantly by the injection and ii) the amplitude and time course of an indicator's fluorescence signal were not substantially different if recorded from a fiber location more distant from the injection site, where the value of $[D_T]$ was smaller. Fibers were studied only if, after injection, they responded in an all-or-none fashion to a brief supra-threshold shock initiated by a pointwise stimulus. The stimulation cathode was typically located ~1 mm from the site of optical recording; thus the propagation time for the action potential to reach the recording site was ~0.5 ms.

F and ΔF

In each experiment, the prestimulus value of fluorescence intensity ("resting" fluorescence, F) and the stimulus-induced change in fluorescence intensity (ΔF) were recorded. In all cases, F was corrected for a component of intensity that was not related to the presence of indicator. This component was measured in each experiment from a fiber region located 1.5–2.5 mm from the injection site, where indicator concentration was negligible. For most measurements, the non-indicator-related intensity was a minor fraction (0.03–0.3) of the indicator-related intensity. All ΔF signals were corrected for a small kinetic delay introduced by the photodiode recording system used to monitor light intensity. This delay, which depended on the value of the feedback resistor used in the current-to-voltage converter of the photodiode system, was usually 0.18 ms but occasionally was 1.8 ms.

Wavelength selections

Excitation at UV wavelengths ($\lambda < 400$ nm) was obtained from a 75-W xenon source (Photon Technology, Princeton, NJ). At visible wavelengths, a 100-W tungsten-halogen source was used, because its output was generally more stable than that of the xenon source. Excitation wavelengths were selected by interference filters of wide bandpass (30–40 nm half-band; Omega Optical Co., Brattleboro, VT, or Chroma Technology, Brattleboro, VT) positioned in the light path before the experimental chamber; λ_{ex} values denote the central wavelength of these filters. The emission filters, positioned after the chamber, were also of wide bandpass (typically, 60–100 nm half-band); λ_{em} values denote the cut-on wavelengths of these filters. With several of the indicators (furaptra, mag-indo-1, and mag-fura-5), a λ_{ex} of 410 nm was used even though this wavelength does not maximize the amplitude of the F and ΔF signals. A λ_{ex} of 410 nm does, however, permit a straightforward estimation of Δf_{CaD}, the change in the fraction of the indicator in the Ca^{2+}-bound form that results from fiber activity. This follows because, at 410 nm, the Ca^{2+}-bound forms of these indicators make little contribution to the measured fluorescence, and Δf_{CaD} is approximately equal to $-\Delta F/F$ (cf. Baylor and Hollingworth, 1988; Konishi et al., 1991; and examples discussed in Results).

Movement artifacts

Throughout the Results, comparisons are made of kinetic parameters (e.g., time to peak and half-width) of ΔF signals from the various indicators. For these comparisons to be meaningful, it is important that movement artifacts in the optical records be small. In spite of the precautions mentioned above to minimize fiber movement, measurements with some indicators (particularly those with small myoplasmic diffusion constants; see Results) sometimes showed small humps or inflections in the falling phase of ΔF that were attributed to movement artifacts. The likely source of these artifacts was a small axial displacement of the fiber caused by some residual tension generated near the tendon ends, where sarcomere length is shorter than in the middle of the fiber (Huxley and Peachey, 1961). Because indicator concentration varies with distance from the injection site, an axial displacement will change the number of indicator molecules, and hence fluorescence,

within the optical field. Movement artifacts were recognized as such because a) they were not always seen in other fibers injected with the same indicator, b) their amplitude and polarity relative to that of the Ca^{2+}-related ΔF varied with the axial distance from the injection site, and c) their presence could be reduced or eliminated by an additional stretch of the fiber. In general, all ΔF traces analyzed for the tables and figures of this article were taken from traces thought to be minimally influenced by movement artifacts. However, at the average sarcomere length of the present experiments, 3.9 μm, the amplitude of $\Delta[Ca^{2+}]$ is probably reduced by ~20%, and the time to peak and half-width of $\Delta[Ca^{2+}]$ are probably increased by ~10% and ~30%, respectively, when compared with the values measured at shorter sarcomere lengths, 2.5–3.0 μm (Konishi et al., 1991).

Ratio fluorescence measurements

As described by Grynkiewicz et al. (1985), the ratio of fluorescence measurements made with two different $\lambda_{ex}/\lambda_{em}$ pairs may be used to estimate a Ca^{2+}-related signal that is nominally free of interference from changes in dye content. If, however, the ΔF values recorded with the two $\lambda_{ex}/\lambda_{em}$ pairs (denoted $\Delta F_1/F_1$ and $\Delta F_2/F_2$) are both sensitive to Ca^{2+}, then calculation of a simple ratio signal—either $(\Delta F_1/F_1)/(\Delta F_2/F_2)$ or $(\Delta F_2/F_2)/(\Delta F_1/F_1)$—yields a waveform that is not linearly related to Δf_{CaD} and hence not linearly related to either $\Delta F/F$ signal. A modified ratio signal was therefore sought that would retain a linear proportionality to Δf_{CaD} and permit a meaningful comparison of the time courses of the ratio-corrected waveform and the individual ΔF waveforms. For this purpose, the measured $\Delta F_1/F_1$ and $\Delta F_2/F_2$ signals were combined according to the equation

$$\Delta F'_1/F_1 = \frac{-K(\Delta F_1/F_1 - \Delta F_2/F_2)}{(1 - K + \Delta F_1/F_1 - K\,\Delta F_2/F_2} . \quad (1)$$

Here, $\Delta F'_1/F_1$ (the ratio-corrected signal) denotes the $\Delta F_1/F_1$ signal that would have been measured if the number of indicator molecules within the optical recording site had remained constant. The parameter K represents the constant ratio $(\Delta F_1/F_1)/(\Delta F_2/F_2)$ that results if ΔF_1 and ΔF_2 are due to $\Delta[Ca^{2+}]$ alone. The derivation of Eq. 1 (see Appendix), which depends on the assumption that K is different from 1, also yields an expression for $\Delta N/N$, the fractional change in the number of indicator molecules within the optical field:

$$\Delta N/N = \frac{(\Delta F_1/F_1 - K\,\Delta F_2/F_2)}{(1 - K)} . \quad (2)$$

In practice, the value of K to be used in Eqs. 1 and 2 can be readily determined, because onset of the Ca^{2+}-related ΔF's precedes onset of any movement-related ΔF. Fig. 2 illustrates, with BTC, sample $\Delta F_1/F_1$ and $\Delta F_2/F_2$ signals and calculation of the $\Delta F'_1/F_1$ and $\Delta N/N$ waveforms. As explained in the Results, the ratio correction was not applied to mag-fura-red, the other potentially ratioable visible wavelength indicator of this study, because the ΔF signal from mag-fura-red contained an unusual component that did not appear amenable to correction by the ratio technique. (*Note:* the ratio technique cannot be used with the visible wavelength indicators based on "orange" and "green" chromophores (calcium-orange-5N, calcium green, etc.), because the amplitude of the Ca^{2+}-related $\Delta F/F$ is approximately the same with all $\lambda_{ex}/\lambda_{em}$ pairs, i.e., $K \simeq 1$.]

Polarized fluorescence measurements

With some indicators, ΔF waveforms were measured with two different forms of plane polarized light in the excitation and emission beams. These measurements were made as described previously for fura-2 (Konishi et al., 1988), by insertion in the light path of two prism polarizers, one positioned between the light source and the preparation, and the other between the preparation and the photodetector. Each polarizer was used in one of two orientations, to select light polarized either parallel or perpendicular to the fiber axis (denoted 0° and 90°, respectively). This yielded a total of four combinations: 0°/0°, 0°/90°, 90°/0°, and 90°/90° (where / separates the excitation and emission polarizations, respectively). Of the indicators so examined (fura-2, furaptra, fura-red and fluo-3 in previous studies; BTC, calcium orange, calcium-orange-5N, calcium-green-5N, magnesium orange, magnesium green, and mag-fura-red in this study), only mag-fura-red revealed a ΔF waveform that varied significantly with polarized light.

Estimation of Δf_{CaD} from absorbance measurements

In a few experiments with BTC, calcium-green-5N and mag-fura-red, the quantity of indicator injected was sufficient to permit an estimation of Δf_{CaD} from absorbance measurements. In general, in vitro absorbance calibration constants are considered to be more reliable for estimation of Δf_{CaD} than are fluorescence constants (Kurebayashi et al., 1993; see also Konishi et al., 1988). For the absorbance measurements, the fiber was illuminated with a small spot of light (diameter, 45–60 μm), and $A(\lambda)$, the resting isotropic absorbance of the indicator (Baylor et al., 1982a), was estimated from 0° and 90° polarized light intensities transmitted in the absence and presence of the fiber. For these measurements, pairs of identical narrowband filters (10 nm half-width, $430 \leq \lambda \leq 570$ nm) were positioned in the light path before and after the experimental chamber. Correction for the fiber's intrinsic absorbance, $A_i(\lambda)$, was made as previously described (e.g., Konishi and Baylor, 1991), based on measurements at a longer wavelength ($\lambda = 600$ nm), where the indicator has no absorbance. $\Delta A(\lambda)$, the stimulus-induced change in isotropic absorbance of the indicator, was estimated from $\Delta I(\lambda)/I(\lambda)$, the fractional change in light intensity transmitted by the fiber (Konishi and Baylor, 1991). The $\Delta A(\lambda)$ measurements were corrected for the fiber's intrinsic absorbance change, $\Delta A_i(\lambda)$. Because absorbance was measured with both 0° and 90° polarized light, it was also possible to check for indicator-related dichroic signals during activity. These signals, which arise if $\Delta A_0 - \Delta A_{90}$ is different from zero, are presumed to reflect activity of indicator molecules bound to one of the oriented structures of myoplasm (Baylor et al., 1982a).

Values of $[D_T]$ were estimated from the values of $A(\lambda)$ by means of Beer's law and the following myoplasmic values of $\epsilon_D(\lambda)$ (the molar extinction coefficient, in units of M^{-1} cm^{-1}, of the Ca^{2+}-free form of the indicator): for BTC, $\epsilon(470) = 33{,}300$; for calcium-green-5N, $\epsilon(510) = 85{,}000$; for mag-fura-red, $\epsilon(450) = 17{,}600$. For the calculations of $\Delta[CaD]$ (the change in the myoplasmic concentration of Ca^{2+}-indicator complex), the following values were used for $\Delta\epsilon_{CaD}(\lambda)$ (the change in molar extinction coefficient with Ca^{2+} complexation): for BTC, $\Delta\epsilon(470) = -29{,}850$; for calcium-green-5N, $\Delta\epsilon(470) = -12{,}000$; for mag-fura-red, $\Delta\epsilon(480) = -17{,}000$. These values were estimated from the indicators' in vitro absorbance spectra redshifted by 12 nm for BTC, 8 nm for calcium-green-5N, and 2 nm for mag-fura-red (the redshift values detected in the analysis of $A(\lambda)$ and $\Delta A(\lambda)$; cf. Results). The extinction coefficients used for mag-fura-red are based on the assumption that f_{MgD}, the fraction of the indicator bound with Mg^{2+} at rest, was 0.2. Δf_{CaD} was then estimated by the ratio $\Delta[CaD]/[D_T]$.

Simultaneous use of two indicators

In several experiments, furaptra and a second indicator were injected into the same region of a fiber, and ΔF signals from the two indicators were measured simultaneously. For these experiments, $\lambda_{ex}/\lambda_{em}$ pairs were chosen to minimize any fluorescence contamination from the other indicator (410/480 for furaptra, 525/590 for calcium-orange-5N and magnesium orange, and 480/510 for calcium-green-5N and magnesium green). Signals were corrected for any remaining contamination, which was estimated in separate experiments on fibers injected with one indicator only.

From the amplitude and time course of $\Delta[Ca^{2+}]$, which can be estimated from furaptra's ΔF (see Results), it is possible to estimate the effective myoplasmic value of k_{+1} and k_{-1} of the second indicator. The method for estimation of the rates (cf. Figs. 3 *B* and 8 *B*) is similar to that described previously in the analysis of optical signals measured

simultaneously with one higher-affinity and one lower-affinity indicator (Baylor et al., 1985a; Klein et al., 1988; Baylor and Hollingworth, 1988; Harkins et al., 1993). As applied here, the method assumes that ΔF values from both indicators reflect a 1:1 reaction with Ca^{2+} and that furaptra's ΔF occurs without kinetic delay (Konishi et al., 1991). The estimate of k_{+1} depends inversely on the myoplasmic value assumed for the $K_{D,\,Ca}$ of furaptra (= 100 μM), which is somewhat uncertain.

AM loading

In one experiment (described in connection with Fig. 6), a fiber was exposed for a period of 137 min to Ringer's containing 10 μM of the AM form of mag-fura-red (plus 0.1% dimethyl sulfoxide). At the end of this time, the entire fiber contained a stable concentration of several hundred micromolar mag-fura-red (Zhao et al., 1995). (This result stands in contrast to the time-varying, spatially localized concentration of indicator that results from the microinjection technique.) This fiber was then exposed to Ringer's containing 4 μM BAPTA-AM (plus 0.2% dimethyl sulfoxide), and changes in the mag-fura-red ΔF signal were monitored as the fiber became progressively loaded with BAPTA.

Estimation of the percentage of indicator bound to myoplasmic constituents

Indicator binding to myoplasmic constituents of low mobility (e.g., soluble and structural proteins) was estimated from the indicator's apparent diffusion constant in myoplasm (D_{app}; cf. column 6 in Table 3 and column 2 in Table 4). A reduction in D_{app} below that expected for a freely diffusible compound of a similar molecular weight is presumed to reflect such binding (cf. Kushmerick and Podolsky, 1969; Maylie et al., 1987a,b,c), and the percentage of bound indicator was estimated under the assumption that the bound molecules are effectively immobile. D_{app} was estimated by the method described previously, from a fit of the one-dimensional diffusion equation to the resting fluorescence intensities measured at times >40 min after the injection and at distances up to 1.5 mm from the injection site (e.g., Baylor and Hollingworth, 1988; Konishi et al., 1991; see also Blinks et al., 1978). To estimate the expected value of D_{app} for a freely diffusible molecule of a given molecular weight (denoted D'_{app}; units of 10^{-7} cm^2 s^{-1}), the following empirical formula was used: $D'_{app} = 58.4 \times (MW)^{-0.213}$. The coefficient and exponent in this formula were selected from a fit of the data of Maylie et al. (1987a,b,c) for the free myoplasmic diffusion of tetramethylmurexide, antipyrylazo III, and arsenazo III (molecular weights of 322, 746 and 776, respectively) and the data of Kushmerick and Podolsky (1969) for the free myoplasmic diffusion of sorbitol, sucrose and ATP (molecular weights of 182, 342 and 507, respectively; diffusion constants referred to 16°C). The bound percentage was then estimated as $100 * (1 - D_{app}/D'_{app})$. (*Note:* based on the same empirical formula, the following estimates for the bound percentages of other Ca^{2+} indicator dyes in intact single fibers can be calculated from previously published values of D_{app} at 16°C: PDAA, 40%; furaptra, 58%; fura-2, 76%; antipyrylazo III, 85%; fluo-3, 87%; fura red, 89%; arsenazo III, 92%; azo1, 93%.)

Data sampling and analysis

AD and DA conversion were carried out with commercial hardware (IDA15125 and PGA/Z units; Indec Systems, Capitola, CA) interfaced to an IBM-compatible computer. Each data collection period began with the opening of an electronically controlled shutter and the recording of the resting light intensity. Then, up to four multiplexed signals were recorded over time: the stimulus artifact, the change in fiber tension, and either a) the change in fiber fluorescence or b) the changes in transmitted light intensity of 0° and 90° polarized light (which were recorded separately with identical photodiode units). The interval between successive data samples was usually 125 μs (or 500 μs for four multiplexed signals), and a 50-ms baseline period preceding fiber stimulation was routinely recorded. Signal amplification before AD conversion was carried out with AM502 amplifiers (Tektronix, Beaverton, OR), with the low-pass filter set at 1 kHz. Data analysis programs were written either in Fortran (Microsoft Corp., Redmond, WA) or in MLAB (Civilized Software, Bethesda, MD). Figures were prepared with MLAB.

Statistics

Parameter values pertaining to the optical measurements are reported as mean ± SEM. The statistical significance of a difference between means was evaluated with Student's two-tailed t-test, with the significance level set at $p < 0.05$.

RESULTS

General considerations

The primary approach used in this paper to evaluate an indicator was to compare its ΔF response triggered by a single action potential with that of furaptra, a lower-affinity, tricarboxylate indicator that is thought to give accurate information about the time course of $\Delta[Ca^{2+}]$. Calibration of the amplitude of $\Delta[Ca^{2+}]$ from furaptra's fluorescence signal is thought to be approximately correct if based on an intracellular value of $K_{D,\,Ca}$ of 100 μM (rather than the 44 μM value measured in vitro; Table 1). With the 100 μM value, the amplitude of $\Delta[Ca^{2+}]$ is similar to that which would have been estimated with PDAA (Konishi et al., 1991; see Introduction).

To compare the time course of indicator signals, values of time to peak and half-width of ΔF are reported. The values from a lower-affinity indicator with rapid reaction kinetics are expected to be very similar to those of furaptra. With a higher-affinity indicator that responds rapidly to $\Delta[Ca^{2+}]$, ΔF will have a broader half-width, because of greater saturation of the indicator with Ca^{2+}, but the time to peak should not be delayed. In contrast, an indicator that is kinetically limited will have a time to peak that is slower than that of furaptra, as well as a broader half-width. Additionally, any component in the ΔF response that does not reflect a simple kinetic reaction between indicator and Ca^{2+} may alter both the time to peak and the half-width of ΔF.

The results for each indicator are presented in a similar order. Fig. 1 gives an example of the ΔF signal recorded with the indicator after action potential stimulation. Tables 2 and 3 give, for lower-affinity and higher-affinity indicators respectively, the basic properties of the ΔF signals, including peak amplitude, time to peak, and half-width. For the lower-affinity indicators, Table 4 gives, where possible, the estimated myoplasmic values for k_{+1}, k_{-1}, and $K_{D,\,Ca}$, as well as the factor by which $K_{D,\,Ca}$ is changed relative to the in vitro value. Tables 3 and 4 also give the diffusion constant of the indicators in the myoplasm and thereby the estimated percentage of indicator bound to myoplasmic constituents. Signals peculiar to a given indicator, for example those relating to secondary components in the fluorescence signal, are presented with the results from that

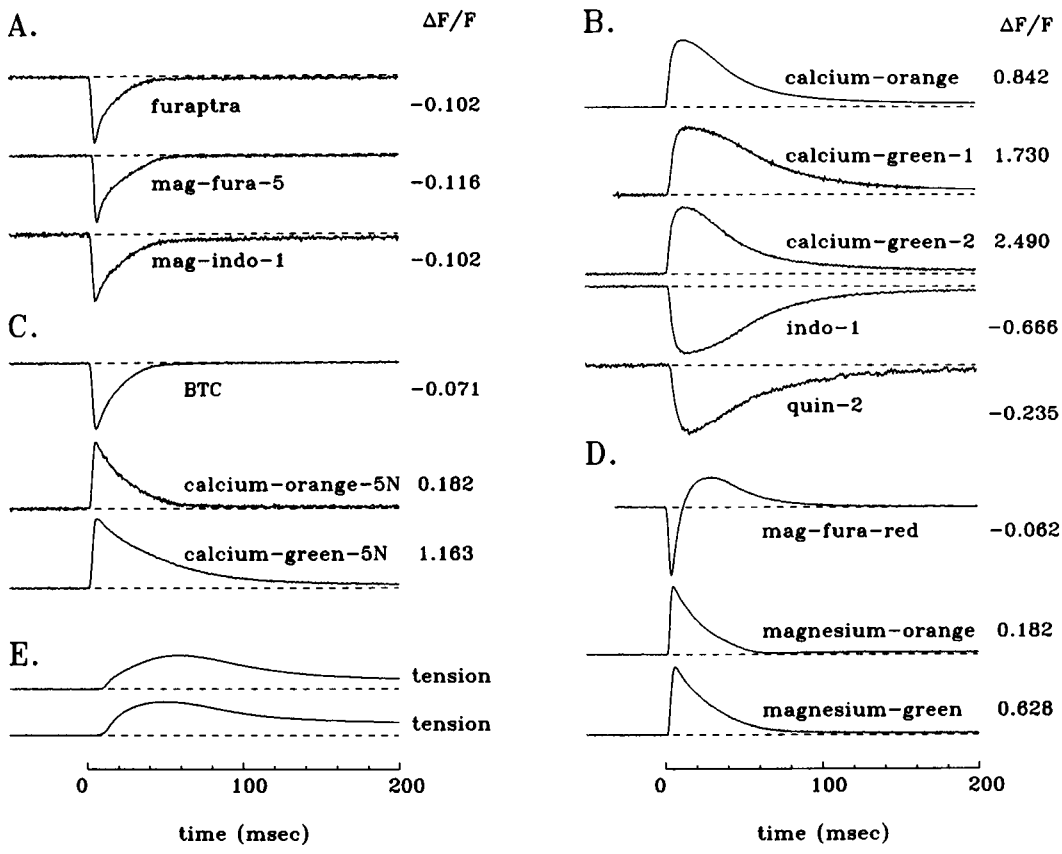

FIGURE 1 The fluorescence change (ΔF) after a single action potential was measured in separate experiments with 14 different Ca^{2+} indicators (*A–D*). In each experiment, a fiber was injected with a single indicator and stimulated at time zero to give an action potential. The indicators fall into four groups: (*A*) Lower-affinity, shorter-wavelength tricarboxylate; (*B*) higher-affinity tetracarboxylate; (*C*) lower-affinity, visible-wavelength tetracarboxylate; (*D*) lower-affinity, visible-wavelength tricarboxylate. Signal amplitudes are normalized to *F*, the value of resting fluorescence measured immediately before stimulation. The peak value of $\Delta F/F$ is indicated beside each trace. (*E*) Records of twitch tension from two representative experiments (the mag-indo-1 experiment in *A* and the indo-1 experiment in *B*); the twitch amplitudes (uncalibrated) are a small fraction of the tension that would have been recorded if the fibers had not been stretched. Records with a shorter pre-stimulus baseline (calcium-green-1 and mag-fura-red) were recorded with a PDP-11 computer. Fiber identification numbers and number of sweeps averaged for the traces shown: furaptra (062295.1, 2), mag-fura-5 (061395.3, 2), mag-indo-1 (051195.1, 2), calcium-orange (051795.1, 2), calcium-green-1 (110691.2, 1), calcium-green-2 (071194.1, 3), indo-1 (062994.2, 2), quin-2 (071594.2, 2), BTC (062995.2, 1), calcium-orange-5N (053195.1, 2), calcium-green-5N (071895.1, 2), mag-fura-red (072993.2, 2), magnesium-orange (050495.2, 1), magnesium-green (052595.1, 2).

indicator. The indicators fall naturally into four groups: higher-affinity tetracarboxylates (cf. Fig. 1 *B*), lower-affinity tetracarboxylates (cf. Fig. 1 *C*), lower-affinity tricarboxylates with principal absorbance bands at UV wavelengths (cf. Fig. 1 *A*), and lower-affinity tricarboxylates with principal absorbance bands at visible wavelengths (cf. Fig. 1 *D*).

Lower-affinity tricarboxylates with principal absorbance bands at UV wavelengths

Furaptra

As shown in columns 3 and 4 of Table 2, the average values for time to peak and half-width of furaptra's ΔF were 5.0 and 10.9 ms, respectively. These average values are essentially identical to those found by Konishi et al. (1991), 5.1 and 9.5 ms. (*Note:* the 5.1 ms value for time to peak quoted here has been reduced from the 6.3 ms value given in Table 3 of Konishi et al., 1991; this reduction corrects for an effect of Ringer Ca^{2+} concentration, which was 11.8 mM in Konishi et al. versus 1.8 mM in this article—see Fig. 8 of Konishi et al. and associated discussion.) On the other hand, the average peak value of furaptra's $\Delta F/F$ in Table 2, -0.132 ± 0.007, is significantly larger than that reported by Konishi et al. (1991), -0.088 ± 0.005. This difference likely reflects biological variation in the average amplitude of $\Delta[Ca^{2+}]$ among different batches of frogs; the reason for this variation is not known. (*Note:* Konishi et al. give an average amplitude of -0.090 with $\lambda_{ex}/\lambda_{em} = 420/480$; this value was adjusted above to -0.088 for comparison with the measurements of this paper, which utilized a $\lambda_{ex}/\lambda_{em} = 410/480$.)

In vitro calibrations with furaptra indicate that $(\Delta F/F)_{max}$ (the value of $\Delta F/F$ that would be observed if Δf_{CaD} were 1.0) is -0.932 with a $\lambda_{ex}/\lambda_{em}$ of 410/480 nm. Given this information, the $\Delta F/F$ signal from furaptra is readily scaled

TABLE 2 Properties of fiber fluorescence signals measured with lower-affinity Ca^{2+} indicators

Indicator ($\lambda_{ex}/\lambda_{em}$) (nm/nm) (1)	N (2)	ΔF Time to peak (ms) (3)	ΔF Half-width (ms) (4)	ΔF Peak ($\Delta F/F$) (5)	$\frac{\Delta F_{steady}}{\Delta F_{peak}}$ (6)	$\frac{\Delta[Ca^{2+}]_{steady}}{\Delta[Ca^{2+}]_{peak}}$ (7)
A. Tetracarboxylates						
BTC (410/480 & 480/510)	6	6.3 ± 0.3	16.2 ± 1.0	0.144* ± 0.006	0.025 ± 0.005 (5)	0.021 ± 0.004 (5)
Calcium-orange-5N (525/590)	5	6.2 ± 0.3	16.8 ± 1.5	0.260 ± 0.041	0.015 ± 0.005 (4)	0.012 ± 0.004 (4)
Calcium-green-5N (480/510)	6	6.3 ± 0.2	36.7 ± 4.5	0.835 ± 0.094	—	—
B. Tricarboxylates ($\lambda_{ex} \leq 420$ nm)						
Furaptra (410/480)	12	5.0 ± 0.1	10.9 ± 0.7	−0.132 ± 0.007	0.044 ± 0.005 (11)	<0.039 ± 0.004 (11)
Mag-fura-5 (410/480)	2	4.9 ± 0.1	9.8 ± 1.5	−0.119 ± 0.003	0.022	<0.019
Mag-indo-1 (410/480)	3	5.2 ± 0.4	11.6 ± 2.3	−0.114 ± 0.010	0.041 ± 0.029 (2)	<0.036 ± 0.025 (2)
C. Tricarboxylates ($\lambda_{ex} \geq 420$ nm)						
Mag-fura-red (480/550)	8	two-component signal (see text)			—	—
Magnesium orange (525/590)	3	5.0 ± 0.0	12.5 ± 2.5	0.145 ± 0.024	0.018 ± 0.009 (3)	<0.015 ± 0.008 (3)
Magnesium green (480/510)	4	6.1 ± 0.4	22.6 ± 2.5	0.507 ± 0.065	0.032 ± 0.004 (3)	<0.015 ± 0.002 (3)

Column 1 lists the indicators and the $\lambda_{ex}/\lambda_{em}$ pairs used for the fluorescence measurements. Column 2 gives the number of experiments in which ΔF was measured, and columns 3–5 summarize the properties of ΔF in response to a single action potential (mean values ± SEM). The quanitities in columns 6 and 7 are defined in the last section of the Results.

*For BTC the amplitude of the ratio signal has been referred to 410/480 nm; if referred to 480/510, the amplitude was −0.072 ± 0.006. For columns 6 and 7, the number of experiments in the calculation of means and SEMs is given in parentheses next to SEM. In columns 6 and 7, values are not given for calcium-green-5N and mag-fura-red because of interference from the slow components of ΔF (see text), and, in the case of mag-fura-5, the values were determined for a single experiment only. For the tricarboxylate indicators, the numbers in column 7 represent an upper limit for $\Delta[Ca^{2+}]_{steady}/\Delta[Ca^{2+}]_{peak}$ because of a likely contribution from $\Delta[Mg^{2+}]$ (see text).

to units of Δf_{CaD} (the change in the fraction of the indicator in the Ca^{2+}-bound form that results from fiber activity). Thus, the average peak value of −0.132 for $\Delta F/F$ (Table 2) corresponds to a peak value of 0.142 for Δf_{CaD}. This latter value, in combination with the 1:1 binding equation and the assumption of an effective myoplasmic value of 100 μM for furaptra's $K_{D,\,Ca}$, corresponds to a peak value of 16.5 μM for $\Delta[Ca^{2+}]$. Figs. 3 *B* and 8 *B* (described in detail below) give examples of $\Delta[Ca^{2+}]$ calculated from furaptra's $\Delta F/F$.

Although previous work (Konishi et al., 1991) indicates that furaptra's ΔF responds to $\Delta[Ca^{2+}]$ without kinetic delay, no experimental estimates have been obtained in vivo or in vitro for k_{+1} and k_{-1}. It seems likely, however, that furaptra's myoplasmic value of k_{-1} is at least 5000 s^{-1} at 16°C. This estimate is based on i) the myoplasmic value of k_{-1} estimated for fura-2, ~20 s^{-1} (Baylor and Hollingworth, 1988; Hollingworth et al., 1992); ii) the ratio of the in vitro values of $K_{D,\,Ca}$ for furaptra and fura-2, ~250; and

TABLE 3 Properties of fiber fluorescence signals measured with higher-affinity Ca^{2+} indicators

Indicator ($\lambda_{ex}/\lambda_{em}$) (nm/nm) (1)	N (2)	ΔF Time to peak (ms) (3)	ΔF Half-width (ms) (4)	ΔF Peak ($\Delta F/F$) (5)	D_{app} ($\times 10^{-7}$ cm^2 s^{-1}) (6)	Myoplasmic binding (%) (7)
Calcium-green-1 (480/510)	2	15.0 ± 1.0	67.1 ± 6.0	1.82 ± 0.09	0.8 ± 0.1	94 ± 1
Calcium-green-2 (480/510)	1	12.0	43.7	2.34	0.6	95
Calcium orange (525/590)	2	14.0 ± 2.0	37.9 ± 2.5	0.691 ± 0.151	1.6 ± 0.5	88 ± 3
Indo-1 (360/470)	2	14.0 ± 0.5	61.5 ± 6.3	−0.67*	2.9 ± 0.8	81 ± 5
Quin-2 (380/480)	2	14.7 ± 1.4	53.4 ± 5.1	−0.235‡	7.8	49

Column definitions 1–5 are the same as in Table 2. Column 6 lists the indicators' apparent diffusion constant in myoplasm; for indicators that had only a single measurement of D_{app}, no SEM is given. Column 7 lists the percentage of indicator bound to immobile myoplasmic constituents (estimated from the values of D_{app} by the formula given in Materials and Methods).

*With indo-1, the peak $\Delta F/F$ was determined with 360/470 illumination in one experiment only; in the other experiment, $\lambda_{ex}/\lambda_{em}$ was 410/480 and $\Delta F/F$ was −0.66.

‡With quin-2, peak $\Delta F/F$ was reliably determined in one experiment only; in the other experiment, uncertainty about the value of non-indicator-related intensity rendered unreliable the estimation of F (and hence $\Delta F/F$).

TABLE 4 Myoplasmic properties of the lower-affinity Ca^{2+} indicators

Indicator (1)	D_{app} (10^{-7} cm^2 s^{-1}) (2)	Myoplasmic binding (%) (3)	k_{+1} (10^7 M^{-1} s^{-1}) (4)	k_{-1} (s^{-1}) (5)	$K_{D,Ca}$ (μM) (6)	$\frac{K_{D,Ca}\text{ (in vivo)}}{K_{D,Ca}\text{ (in vitro)}}$ (7)
A. Tetracarboxylates						
BTC	0.71 ± 0.04, (4)	95 ± 1	0.5	1000	188	7.2
Calcium-orange-5N	1.4 ± 0.1, (3)	89 ± 1	≤1.2	1040	≥87	≥1.6
Calcium-green-5N	1.2 ± 0.2, (3)	91 ± 1	(0.6)	(1000)	156	2.5
B. Tricarboxylates ($\lambda_{ex} \leq 420$ nm)						
Furaptra	[6.8 ± 0.2, (6)]	58 ± 2	≥5.0	≥5000	100	2.3
Mag-fura-5	7.8	57	—	≥5000	—	—
Mag-indo-1	4.4	73	—	≥5000	—	—
C. Tricarboxylates ($\lambda_{ex} \geq 420$ nm)						
Mag-fura-red	2.9 ± 0.2, (3)	82 ± 2	≥2.1	≥5000	242	4.4
Magnesium orange	2.3 ± 0.1, (3)	84 ± 1	—	≥2500	—	—
Magnesium green	1.5	90	≤9.0	1750	≥19	≥2.8

Column 2 gives the mean value of the indicator's apparent diffusion constant in myoplasm, with the SEM and the number of experiments indicated in parentheses (if the measurement was made in more than one experiment). For furaptra, values in square brackets were taken from Konishi et al. (1991). Column 3 gives the percentage of the indicator bound to immobile myoplasmic constituents, estimated from the values of D_{app} as described in Materials and Methods. Columns 4 and 5 give the estimated values of k_{+1} and k_{-1} in myoplasm and column 6 gives the myoplasmic estimate of $K_{D,Ca}$. Column 7 gives column 6 divided by the value of $K_{D,Ca}$ listed in Table 1.

Notes concerning column 4: With BTC, calcium-green-5N, furaptra and mag-fura-red, k_{+1} was calculated from columns 5 and 6 and the formula $k_{+1} = k_{-1}/K_D$; with calcium-orange-5N and magnesium green, k_{+1} was estimated by the method illustrated in Figs. 3 *B* and 8 *B*; the value of k_{+1} estimated for magnesium green is considered an upper limit because the value assumed for Δf_{CaD} (0.5) is likely to represent an upper limit.

Notes concerning column 5: k_{-1} for the rapidly reacting indicators (furaptra, mag-fura-5, mag-indo-1, and mag-fura-red) is assumed to be at least 5000 s^{-1} (see second section of Results). k_{-1} values for calcium-orange-5N and magnesium green were estimated by the method illustrated in Figs. 3 *B* and 8 *B*. The value for BTC is assumed to be similar to that of calcium-orange-5N (see text). The value for the faster component of ΔF from calcium-green-5N is also assumed to be similar to that of calcium-orange-5N but, as indicated by parentheses, is less certain because of contamination by the slower component of ΔF (see text).

Notes concerning column 6: With BTC, calcium-green-5N, and mag-fura-red, $K_{D,Ca}$ was estimated from Δf_{CaD} (measured by absorbance) and the average amplitude of $\Delta[Ca^{2+}]$ estimated with furaptra. With calcium-orange-5N and magnesium green, a similar method was used, except that the values of Δf_{CaD} were assumed, not measured (see text). With furaptra, the value of $K_{D,Ca}$ was taken from Konishi et al. (1991). Dashes in columns 4–7 indicate that insufficient information was available to make an estimate.

iii) the observation that values of k_{-1} for tetracarboxylate indicators scale in approximate proportion to $K_{D,Ca}$, at least under in vitro conditions (Kao and Tsien, 1988; Lattanzio and Bartschat, 1991). Two other observations suggest that furaptra's k_{-1} might be severalfold larger than 5000 s^{-1}. First, the comparisons mentioned in the Discussion suggest that, for indicators with similar values of $K_{D,Ca}$, reaction rates of tricarboxylates may be faster than those of tetracarboxylates. Second, indicator binding to myoplasmic constituents appears to reduce reaction rates, and the degree of binding appears to be less for furaptra than for fura-2 (Konishi et al., 1991). Under the assumption that furaptra's myoplasmic value of $K_{D,Ca}$ is 100 μM and that k_{-1} is at least 5000 s^{-1}, k_{+1} is calculated to be at least 5×10^7 M^{-1} s^{-1} (cf. columns 4–6 of Table 4).

Mag-fura-5

In frog single fibers loaded with the AM form of mag-fura-5 and stimulated by an action potential, ΔF at low temperature (3°C) has a time to peak of 15–20 ms and a half-width of ~55 ms (as estimated by us from figures 3 and 4 of Claflin et al., 1994). Based on this indicator's chemical similarity to furaptra and a similar low affinity for Ca^{2+}, these authors assumed that mag-fura-5 tracks $\Delta[Ca^{2+}]$ without delay. The experiments illustrated in Fig. 1 A and summarized in Table 2 confirm this assumption. For mag-fura-5, the average values of time to peak and half-width of $\Delta F/F$ were 4.9 (± 0.1) ms and 9.8 (± 1.5) ms, respectively, whereas that of the peak amplitude was −0.119 (± 0.003) None of these values is significantly different from the corresponding value observed with furaptra. Hence, $\Delta[Ca^{2+}]$ time courses calculated from $\Delta F/F$ of mag-fura-5 and furaptra would also be essentially identical. (*Note:* In vitro absorbance titrations indicate that $(\Delta F/F)_{max}$ at a $\lambda_{ex}/\lambda_{em}$ of 410/480 is probably quite similar for mag-fura-5 and furaptra; hence the amplitude of Δf_{CaD} is probably quite similar.)

Mag-indo-1

Measurements analogous to those just described for mag-fura-5 were also made with mag-indo-1 and yielded essentially identical results (cf. columns 3–5 of Table 2). Thus, mag-indo-1, like furaptra and mag-fura-5, also appears to track $\Delta[Ca^{2+}]$ without delay.

Column 3 of Table 4 shows that the percentage of indicator bound to immobile myoplasmic constituents lies in the range 57–73% for furaptra, mag-fura-5, and mag-indo-1.

No evidence has been obtained, from either polarization (Konishi et al., 1991) or spectral (Konishi et al., 1993) measurements, to suggest the presence of any secondary components to ΔF from indicators of this type.

Higher-affinity tetracarboxylates

For comparative purposes, ΔF values in response to a single action potential were measured with five higher-affinity indicators: calcium-green-1, calcium-green-2, calcium orange, indo-1, and quin-2. These indicators have not been studied previously in intact single fibers of frog. As shown in Table 3, average values for the times to peak of ΔF ranged from 12 to 15 ms and, for the half-widths of ΔF, from 38 to 67 ms. These values, which are similar to those previously observed with fura-2, fura-red, and fluo-3 at nonperturbing concentrations (13–21 ms for times to peak and 47–63 ms for half-widths; Baylor and Hollingworth, 1988; Kurebayashi et al., 1993; Harkins et al., 1993), are markedly slower than the corresponding values observed with furaptra. As with fura-2, fura-red, and fluo-3, the increases in time to peak are presumed to reflect limitations imposed by small effective values of k_{-1} in myoplasm, whereas the increases in half-width are presumed to reflect this limitation plus the nonlinearity associated with a large value of Δf_{CaD}. No attempt was made to obtain quantitative estimates of k_{+1}, k_{-1}, and Δf_{CaD} for the five higher-affinity indicators used in the present study, but they are probably similar to the values previously estimated for fura-2, fura-red, and fluo-3 (Baylor and Hollingworth, 1988; Kurebayashi et al., 1993; Harkins et al., 1993). Thus, with all higher-affinity indicators tested, substantial kinetic corrections are required to extract an accurate time course of $\Delta[Ca^{2+}]$ from ΔF.

Lower-affinity, visible-wavelength tetracarboxylates

BTC ratio fluorescence measurements

BTC, with a fluorophore based on a coumarin moiety, is a ratioable Ca^{2+} indicator (Iatridou et al., 1994). In in vitro measurements with an emission wavelength of 540 nm, the indicator's isosbestic wavelength (λ_{iso}) for fluorescence excitation lies in the range 430–435 nm (figure 1 of Iatridou et al., 1994).

The upper two traces in Fig. 2 show ΔF signals recorded from BTC with 2 $\lambda_{ex}/\lambda_{em}$ pairs: 410/480 nm (trace labeled $\Delta F_1/F_1$) and 480/510 nm (trace labeled $\Delta F_2/F_2$). At early times after stimulation, the 410/480 signal is positive and the 480/510 signal negative, as expected for a rise in $[Ca^{2+}]$. At later times after stimulation, the 410/480 and 480/510 traces in Fig. 2 do not have identical time courses; this indicates a component of ΔF not directly related to $\Delta[Ca^{2+}]$. This component is thought to reflect a movement artifact, and its effects should thus be susceptible to correction by the ratio technique.

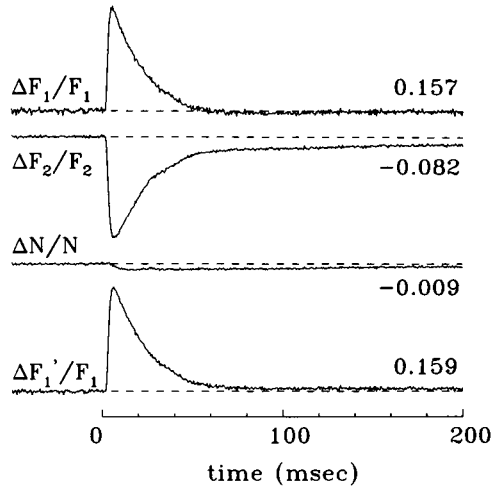

FIGURE 2 Fluorescence signals from BTC. The upper two traces show $\Delta F_1/F_1$ ($\lambda_{ex}/\lambda_{em}$ = 410/480 nm) and $\Delta F_2/F_2$ ($\lambda_{ex}/\lambda_{em}$ = 480/510 nm), as indicated. (*Note:* with our filter set, it was not possible to use the 410/510 combination, because the 510 filter was not blocked sufficiently well to exclude light below 420 nm.) The trace labeled $\Delta N/N$ was obtained from the $\Delta F_1/F_1$ and $\Delta F_2/F_2$ traces with Eq. 2. The scaling factor K (= −2.019) was obtained from a least-squares fit of the $\Delta F_1/F_1$ trace with the $\Delta F_2/F_2$ trace up until 5.5 ms after stimulation, i.e., through the time when $\Delta[Ca^{2+}]$ alone is thought to contribute to the ΔF's. $\Delta N/N$ is presumed to reflect a small movement of the fiber, which changed the number of indicator molecules within the optical field. (*Note:* given i) the value of BTC's diffusion constant (column 2 of Table 4) and ii) the time and location of the measurements in Fig. 2 (~13 min after injection; fluorescence collected from a 300 μm length of fiber centered ~20 μm from the injection site), calculations indicate that a $\Delta N/N$ of amplitude −0.009 would result if the fiber movement consisted of an axial displacement of 10 μm.) The trace labeled $\Delta F_1'/F_1$ is the ratio trace calculated with Eq. 1 and represents the Ca^{2+}-related fluorescence change that would have been measured with $\lambda_{ex}/\lambda_{em}$ = 410/480 nm if the fiber had not moved. The peak amplitude of each trace is indicated at the right. The times to peak of the $\Delta F_1/F_1$, $\Delta F_2/F_2$, and $\Delta F_1'/F_1$ traces were 6.0, 6.5, and 6.0 ms, respectively, whereas the half-widths were 15.5, 20.0, and 17.4 ms, respectively. Fiber 050495.1.

The third and fourth traces in Fig. 2 (labeled $\Delta N/N$ and $\Delta F'_1/F_1$) were calculated from Eqs. 1 and 2, with the 410/480 and 480/510 signals serving as $\Delta F_1/F_1$ and $\Delta F_2/F_2$, respectively (cf. legend of Fig. 2). As estimated by the $\Delta N/N$ trace, movement in this fiber caused a small decrease (of peak fractional amplitude, −0.009) in the number of indicator molecules within the optical recording field; the time to peak and half-width of the $\Delta N/N$ trace were ~20 and ~145 ms, respectively. Trace $\Delta F_1'/F_1$, the ratio-corrected trace, provides an estimate of the 410/480 signal that would have been measured if N had not changed. The peak value, time to peak, and half-width of this trace differ slightly from those of the $\Delta F_1/F_1$ trace (see legend of Fig. 2).

An effect of fiber movement in the traces of Fig. 2 was detected even though the fiber was stretched to a sarcomere length of 3.8 μm and lowered onto pedestal supports. Similar movement artifacts at similar sarcomere lengths were seen in the other experiments with BTC, and their presence raises the question whether movement artifacts may also have contaminated the ΔF signals recorded with the other

indicators. With the higher-affinity indicators, the amplitudes of $\Delta F/F$ due to $\Delta[Ca^{2+}]$ were substantially larger than observed with BTC; thus the relative effect of a movement artifact is substantially smaller. Among the lower-affinity indicators, BTC has the smallest value of apparent myoplasmic diffusion constant (D_{app}; column 2 of Table 4). This implies that, at a similar time after injection, the relative gradient in indicator concentration was greater with BTC than with the other lower-affinity indicators. Hence, for a small axial displacement of the fiber (the type of movement observed visually to apply to our fibers), the fractional change in the number of indicator molecules within the optical field was, in general, greater with BTC than with the other indicators. In practice, most of the ΔF measurements summarized in Tables 2–4 were made within 10–30 min after the injection of indicator. At these times, the prominent gradient in resting F that was readily observed near the injection site with BTC was less apparent with the other indicators. For example, with furaptra, which has a ~10-fold larger diffusion constant than BTC, there was little gradient in resting F at comparable measurement times. Thus, in general, movement contamination in the ΔF signals was less with the other indicators than with BTC.

Ratio traces analogous to that of Fig. 2 were calculated in the six experiments with BTC. The average values for time to peak and half-width, 6.3 ± 0.3 ms and 16.2 ± 1.0 ms, respectively (Table 2), are both significantly larger than the comparable values observed with furaptra. Because of the overlap in the excitation spectra of BTC and furaptra, it was not practical to attempt a simultaneous measurement of the ΔF signals from both indicators in the same fiber. However, because a) the time to peak of BTC's signal is about 1.3 ms greater than that of furaptra and b) the peak value of BTC's Δf_{CaD} is not large (next paragraph), it is likely that BTC's effective value of k_{-1} in myoplasm is ~1000 s^{-1} at 16°C (cf. results described below for calcium-orange-5N).

Estimation of Δf_{CaD} for BTC

In one experiment (fiber 062995.2), the quantity of BTC injected was somewhat larger than in the other experiments and it was possible to resolve accurately BTC's resting absorbance in myoplasm, $A(\lambda)$, as well as its change in absorbance in response to action potential stimulation, $\Delta A(\lambda)$. A comparison (not shown) of the $A(\lambda)$ and $\Delta A(\lambda)$ spectra with BTC's in vitro spectra revealed the following information: i) The in vivo $A(\lambda)$ and $\Delta A(\lambda)$ spectra were not well fitted by the in vitro spectra unless the latter were redshifted by about 12 nm. A redshift of this magnitude has been observed with other indictor dyes (e.g., a 10-nm shift was observed with phenol red; Baylor and Hollingworth, 1991) and suggests that a large percentage of the indicator is bound to myoplasmic constituents (cf. column 3 of Table 4). ii) At the time of the BTC absorbance measurements (21–27 min after injection), the myoplasmic value of $A(470$ nm) was 0.050, which, based on the molar extinction coefficient given in Materials and Methods and the effective path length of the light in myoplasm (~57 μm), corresponds to a myoplasmic BTC concentration of ~265 μM. iii) In response to an action potential, the peak value of $\Delta A(470)$ was 0.0034, which corresponds to a change in concentration of Ca^{2+}-BTC complex of ~20 μM. iv) The peak value of Δf_{CaD} in this experiment was thus 0.075 (= 20/265). v) A peak Δf_{CaD} of 0.075 is representative of the other experiments with BTC, because the amplitude of the $\Delta F/F$ measurements in this fiber (0.156 at 410/480 and −0.075 at 480/510, estimated at the time of the absorbance measurements) was close to the average value observed in the other BTC experiments (cf. Table 2). vi) If $\Delta[Ca^{2+}]$ is calculated from the peak of Δf_{CaD} and BTC's in vitro value of $K_{D,\,Ca}$ (26 μM; Table 1), a value of 2.1 μM is obtained. This value is ~8-fold smaller than the average amplitude of $\Delta[Ca^{2+}]$ estimated with furaptra under these experimental conditions (see above) and indicates that BTC's effective value of $K_{D,\,Ca}$ in myoplasm is ~8-fold larger than that measured in the in vitro titrations. This large change in the effective value of $K_{D,\,Ca}$ is very likely related to the large percentage of bound BTC molecules in the fiber (~95%; column 3 of Table 4).

An unexpected component of the fluorescence signal from BTC

For calculation of the BTC ratio signal (Fig. 2 and Eqs. 1 and 2 in Materials and Methods), an estimate is required for the parameter K, the ratio of $\Delta F_1/F_1$ to $\Delta F_2/F_2$ that results from a Ca^{2+}-related change. During the time taken for any bracketed series of 410/480 and 480/510 measurements (~1 min), K appeared to be a well-determined constant. On a time scale of tens of minutes, however, a significant change in the value of K was observed in some, but not all, experiments. For example, in fiber 050495.1, K changed from an initial value of −1.97 to a final value of −1.58 (estimated 8 and 115 min after injection, respectively). In another experiment, K changed from −1.79 to −0.97 (10 and 96 min after injection; fiber 050295.2). In contrast, in three other fibers, early and late values of K differed by less than 10%: −1.93 and −1.97 (10 and 63 min; fiber 062695.1), −2.31 and −2.15 (16 and 57 min; fiber 062995.1), and −2.20 and −2.07 (17 and 103 min; fiber 062995.2). In fiber 062995.2, K underwent a late decline, from −2.07 to −1.75 (from 103 to 155 min, respectively), a change that began shortly after a period of extensive fiber stimulation. At the end of all experiments just described, the fibers were still responding to action potential stimulation in an all-or-none fashion.

These systematic changes in K, from more negative to less negative values, did not appear to be related to BTC's concentration in myoplasm. Moreover, the changes did not appear to arise simply from an increase in F_1/F_2 (from less positive to more positive values) or an increase in $\Delta F_1/\Delta F_2$ (from more negative to less negative values), but rather from a combination of both increases. The potential significance of these changes can be illustrated by the increases observed in F_1/F_2 for fibers 050295.2 and 050495.1, which

were 10 and 36%, respectively, from the beginning to the end of the experiments. Remarkably, these increases are comparable to the change in F_1/F_2 produced by a single action potential, when ~0.08 of the BTC molecules complex Ca^{2+} in response to the 10–20 μM rapid rise in free [Ca^{2+}] (see above). For example, for the six BTC experiments summarized in Table 2, the average peak value of $(F_1 + \Delta F_1)/(F_2 + \Delta F_2)$ resulting from a single action potential represents a 29 ± 5% increase in F_1/F_2 above its resting value. Thus it does not seem likely that the slow increments in F_1/F_2 observed for fibers 050295.2 and 050495.1 could simply reflect an increase in resting [Ca^{2+}], because a) from the data just mentioned, this increase would have to have been many micromoles per liter, yet b) these fibers continued to respond throughout the experiment with an all-or-none ΔF of reasonably normal size. (*Note:* With mag-fura-red, the other visible wavelength indicator of this study that is potentially ratioable, values of F_1/F_2 were essentially identical among all fibers and showed no variation for time periods as long as 150 min.)

These results indicate that BTC's fluorescence ratio signal responds to some myoplasmic factor(s) other than [Ca^{2+}]. It is unlikely that this factor is simply a change in myoplasmic pH or free [Mg^{2+}], because in vitro calibrations in a standard buffer solution (not shown) indicate that BTC's fluorescence is insensitive to changes in pH and [Mg^{2+}] in the physiological range. A more likely possibility is that BTC's fluorescence is sensitive to the state of bound indicator molecules. As mentioned earlier, BTC appears to be very heavily bound to myoplasmic constituents, and the possibility exists that BTC's interaction with these constituents may change. For example, late in an experiment, or as a result of prolonged stimulation or fiber damage, pH may fall, energy sources may deplete, and resting levels of [Ca^{2+}] and [Mg^{2+}] may rise. These, and/or other associated changes, may affect the binding, and hence fluorescence (and possibly absorbance), of BTC.

Calcium-orange-5N

As indicated in Table 1, the values of $K_{D,\,Ca}$ for calcium-orange-5N and calcium-green-5N are more than 100-fold larger than those of their parent compounds, calcium-orange and calcium-green-1. These increases result from the addition of an NO_2 group near the tetracarboxylate Ca^{2+}-binding moiety (Molecular Probes) and are likely to arise because of a >100-fold increase in the value of k_{-1}. Thus, these "5N" indicators are expected to respond much more rapidly to $\Delta[Ca^{2+}]$ than are the parent compounds.

Fig. 1 and the data in Tables 2 and 3 confirm that the time course of ΔF from calcium-orange-5N is substantially briefer than that of calcium-orange. For calcium-orange-5N, the average values of time to peak and half-width of ΔF, 6.2 (± 0.3) ms and 16.8 (± 1.5) ms, respectively (Table 2), are both significantly smaller than the corresponding values for calcium-orange, 14.0 (± 2.0) ms and 37.9 (± 2.5) ms, respectively (Table 3). The difference in times to peak

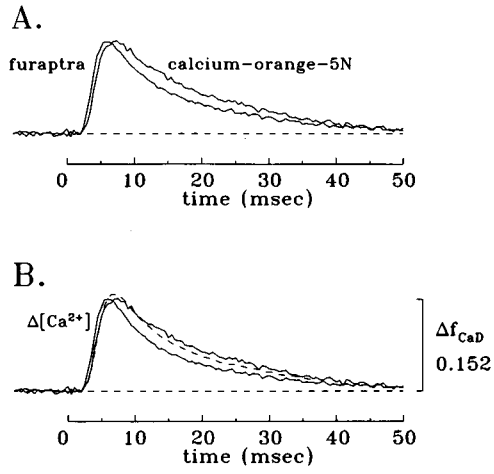

FIGURE 3 (*A*) Values of ΔF measured simultaneously in the same fiber with furaptra and calcium-orange-5N. The furaptra record is the average of single sweeps taken before and after the calcium-orange-5N signal (two sweeps). The peak amplitudes of $\Delta F/F$ were −0.142 (furaptra) and 0.262 (calcium-orange-5N). (*B*) Kinetic fitting of the calcium-orange-5N signal. $\Delta[Ca^{2+}]$ (peak amplitude of 18.0 μM) was obtained from the furaptra signal in *A* by the method described in the text. $\Delta[Ca^{2+}]$ was used to drive a 1:1 Ca^{2+}-binding reaction to give Δf_{CaD}. The dashed line represents Δf_{CaD} best-fitted to the calcium-orange-5N record (reproduced from *A*). A peak amplitude of 0.152 was assumed for Δf_{CaD} (the same as measured for furaptra), and the fitted values were $1.41 \times 10^7\ M^{-1}\ s^{-1}$ for k_{+1} and 1213 s^{-1} for k_{-1}. Fiber 092094.2.

indicates that the effective myoplasmic value of k_{-1} is indeed larger for calcium-orange-5N than that for calcium-orange. However, because the average time to peak of ΔF from calcium-orange-5N is significantly larger than that from furaptra (5.0 ± 0.1 ms; Table 2), the question arises whether calcium-orange-5N tracks $\Delta[Ca^{2+}]$ with some delay.

To answer this question, three experiments were carried out in which furaptra and calcium-orange-5N were coinjected into the same fiber. Fig. 3 shows results from one of these experiments. In Fig. 3 *A*, the time course of furaptra's ΔF (time to peak, 6.0 ms; half-width, 10.1 ms) is clearly briefer than that of calcium-orange-5N (time to peak, 7.3 ms; half-width, 13.7 ms). Very similar results were observed in the other two experiments, with time to peak values for ΔF of 5.0 versus 6.5 ms and 6.0 versus 7.5 ms (furaptra versus calcium-orange-5N, respectively) and half-width values of 15.8 versus 22.1 ms and 10.8 versus 14.4 ms. These results confirm that calcium-orange-5N responds to $\Delta[Ca^{2+}]$ with some delay.

The results of the simultaneous injections can be analyzed to estimate values of k_{+1} and k_{-1} for calcium-orange-5N (see Materials and Methods). $\Delta[Ca^{2+}]$ (Fig. 3 *B*) was calculated from $\Delta F/F$ of furaptra (Fig. 3 *A*), as described in the second section of the Results. The ΔF waveform from calcium-orange-5N (reproduced in Fig. 3 *B*) was then fitted by least-squares adjustment of the values of k_{+1} and k_{-1} assumed for the reaction between Ca^{2+} and calcium-orange-5N. As indicated by the fit in Fig. 3 *B* (*dashed*

trace), the time course of ΔF of calcium-orange-5N is approximately explained if this indicator's myoplasmic values of k_{+1} and k_{-1} are $\sim 1.4 \times 10^7$ M^{-1} s^{-1} and ~ 1200 s^{-1}, respectively (see legend of Fig. 3).

For the fit in Fig. 3 *B*, a peak value of 0.152 was assumed for Δf_{CaD} of calcium-orange-5N. This value was not measured in the experiments but was set to that measured simultaneously for furaptra, based on the similarity of the in vitro values of $K_{D,\ Ca}$ for these two indicators (Table 1). Because of uncertainty in the value of Δf_{CaD} for calcium-orange-5N, values of k_{+1} and k_{-1} were also estimated for three other assumed values for Δf_{CaD}: 0.1, 0.2, and 0.3. In these least-squares fits (not shown), the fitted values of k_{+1} varied, as expected, in proportion to Δf_{CaD}, whereas the estimates of k_{-1} (950 − 1200 s^{-1}) differed only slightly from the estimate obtained in Fig. 3 *B*. Thus, irrespective of the exact value that applies to Δf_{CaD} of calcium-orange-5N, the average value from the four fits indicates that k_{-1} of calcium-orange-5N in this experiment was ~ 1100 s^{-1}.

Fits analogous to those just described were also carried out for the two other experiments that involved coinjection of furaptra and calcium-orange-5N, and the results of the analysis (not shown) were very similar. In these experiments, the average values of k_{-1} estimated for the four assumed values of Δf_{CaD} were 890 and 1010 s^{-1}, whereas the values of k_{+1} estimated under the assumption that Δf_{CaD} was the same for calcium-orange-5N and furaptra were 1.2×10^7 M^{-1} s^{-1} and 1.1×10^7 M^{-1} s^{-1}. The overall conclusion from the three experiments is that calcium-orange-5N's ΔF tracks $\Delta[Ca^{2+}]$ with a small delay, approximately that expected if the effective myoplasmic value of k_{-1} is ~ 1000 s^{-1} (column 5 of Table 4). Estimated values of k_{+1} and $K_{D,\ Ca}$ for calcium-orange-5N are uncertain, however, because no experimental estimate was obtained for Δf_{CaD}.

(*Notes:* 1) In each of the experiments just described, the best fit of calcium-orange-5N's ΔF was obtained under the assumption that its Δf_{CaD} was 0.3. It seems unlikely, however, that Δf_{CaD} was larger than the value measured for furaptra in the same experiment (average value, 0.175; $N = 3$). This follows because, in vitro, calcium-orange-5N has a larger value of $K_{D,\ Ca}$ and, in vivo, a larger fraction of the calcium-orange-5N molecules appear to be bound to myoplasmic constituents (cf. column 3 of Table 4). A possible explanation for the finding that a larger value of Δf_{CaD} gave a better fit is that a slower, secondary component broadens the time course of ΔF from calcium-orange-5N. Because an increased level of saturation is associated with a broader signal response, a two-component signal analyzed by the method of Fig. 3 would be better fitted with a larger value of Δf_{CaD}. A slower component of this type is clearly identified in the ΔF signal of calcium-green-5N (next section). 2) A technical problem observed with calcium-orange-5N, but not with the related indicator magnesium orange, was a reduction in the amplitude of $\Delta F/F$ due to illumination. With the standard method of excitation of calcium-orange-5N (a 500–550-nm wide-band filter in combination with the 100-W tungsten-halogen source), 5 s of illumination decreased the amplitude of ΔF by $\sim 20\%$ (average of three experiments), with little or no effect on F. In contrast, in another experiment (fiber 092094.1), which used an excitation band of 465–495 nm, there was no detectable change in signal amplitude after 35 s of illumination. With 465–495 nm excitation, however, two effects combine to reduce substantially the amount of light absorbed by calcium-orange-5N: i) the integrated intensity at the fiber is substantially less with 465–495 nm illumination, because a) the output of the source is less at the shorter wavelengths and b) the half-width of the 480 nm excitation filter was 30 nm rather than 50 nm; and ii) $A(\lambda)$ of the indicator averaged over the 465–495-nm band is $\sim$3-fold less than over the 500–550-nm band.)

Calcium-green-5N

Fig. 1 suggests that the time to peak of ΔF of calcium-green-5N is also significantly briefer than that of its higher-affinity parent compound, calcium-green-1. Indeed, the average time to peak value of calcium-green-5N, 6.3 ± 0.2 ms (Table 2), is significantly smaller than that of calcium-green-1, 15.0 ± 1.0 ms (Table 3). However, the value for calcium-green-5N, which is very similar to that observed for BTC and calcium-orange-5N, is significantly larger than that for furaptra. As for BTC and calcium-orange-5N, the comparison with furaptra indicates that ΔF from calcium-green-5N tracks $\Delta[Ca^{2+}]$ with some delay. A surprising property of the ΔF from calcium-green-5N, however, is that its average value of half-width, 36.7 ± 4.5 ms (Table 2), is more than twice the corresponding values for BTC and calcium-orange-5N. Both of these differences are statistically significant.

One possible explanation for the broad half-width of the calcium-green-5N signal is that this indicator becomes heavily saturated with Ca^{2+} during activity. Initial support for this possibility was obtained in two coinjection experiments with furaptra. In both experiments, the peak amplitude, time to peak, and half-width of the ΔF signals from the indicators were in agreement with the values expected from Table 2 (−0.132, 5.0 ms, and 8.3 ms, respectively, for furaptra and 0.964, 6.5 ms, and 36.5 ms for calcium-green-5N, fiber 101494.1; and −0.133, 5.5 ms, and 16.4 ms for furaptra and 0.484, 8.0 ms, and 58.2 ms for calcium-green-5N, fiber 101494.1), and the broad time course of the ΔF signals from calcium-green-5N was well fitted from the measurements of $\Delta[Ca^{2+}]$ with furaptra if the assumption was made that Δf_{CaD} for calcium-green-5N was 0.7–0.8. These large values of Δf_{CaD} were considered unlikely, however, because the implied intracellular value of $K_{D,\ Ca}$ for calcium-green-5N (~ 30 μM) is substantially smaller than the in vitro value (63–85 μM; Table 1). With other indicators that have a large percentage of bound indicator, intracellular values of $K_{D,\ Ca}$ are larger, not smaller, than the in vitro values (cf. columns 3 and 7 of Table 4).

To further test this hypothesis, two experiments were carried out with calcium-green-5N alone that involved injection of sufficiently large myoplasmic concentrations of indicator (estimated values, 89 μM in fiber 072095.1 and 109 μM in fiber 072095.2) to permit a direct estimation of Δf_{CaD} by means of absorbance measurements. The peak values of Δf_{CaD} estimated in the two experiments were small, 0.078 and 0.101. Moreover, the peak values of $\Delta F/F$ (0.642 and 1.019, respectively) and the half-width values of ΔF (49.87 ms and 27.6 ms) were about as expected from the average value given in Table 2. Thus, the broad half-width of ΔF is not related to heavy saturation of the indicator with Ca^{2+}. (*Note:* In fiber 072095.1, the estimate of resting $A(510)$ was 0.0316 and the peak of $\Delta A(430)$ in response to an action potential was -0.00035; hence the ratio $\Delta A(430)/A(510)$ was -0.0111, a value 0.078 times that measured in the in vitro absorbance titrations for a Δf_{CaD} of 1.0. In fiber 072095.2, resting $A(510)$ was 0.0563 and the peak of $\Delta A(430)$ in response to an action potential was -0.00080, thus $\Delta A(430)/A(510)$ was -0.0142, a value 0.101 times the maximum value. If the average amplitude of $\Delta[Ca^{2+}]$ is calibrated from the amplitude of Δf_{CaD} and an in vitro value of 63 μM for $K_{D,\,Ca}$ (Table 1), a value of 6.2 μM is obtained. Because this value is two- to threefold smaller than the 16.5 μM estimated with furaptra (see above), it follows that the in vivo value of $K_{D,\,Ca}$ for calcium-green-5N is two- to threefold larger than that given in Table 1 (cf. column 7 of Table 4).)

Because calcium-green-5N is not heavily saturated with Ca^{2+}, the broad half-width of its ΔF must arise from the presence of a slow component in the signal. This component cannot be a movement artifact because similarly large half-width values were observed in fibers stretched to sarcomere lengths of 4.3 μm, where fiber movement was negligible (e.g., fiber 072095.1, ΔF half-width of 54.7 ms). Rather, as with the slow component of the ΔF signal from mag-fura-red (described in detail below), the slow component of the calcium-green-5N signal must reflect some event not directly related to a simple Ca^{2+}:indicator reaction. These slow components of ΔF are reminiscent of the slow dichroic components of the absorbance signals detected with the metallochromic dyes arsenazo III and dichlorophosphonazo III (Baylor et al., 1982a).

To study further the slow component of the calcium-green-5N signal, two other types of measurements were made, which yielded some additional information but not a conclusive characterization: i) In both of the absorbance experiments with calcium-green-5N mentioned above, the ΔA measurements revealed the presence of a small indicator-related dichroic signal. The amplitude of this signal was similar to that previously detected in an analogous experiment with fluo-3 (figure 6 *A* of Harkins et al., 1993), and, as with fluo-3, the onset of the dichroic signal lagged slightly behind the onset of the isotropic ΔA. Interestingly, because $\Delta A_0(\lambda) - \Delta A_{90}(\lambda)$ is negative for calcium-green-5N and fluo-3 (at $480 \leq \lambda \leq 520$, the wavelengths where the signals were well resolved), the direction of the dichroic signal is opposite that of the dichroic signal seen with the metallochromic dyes (Baylor et al., 1982a). Thus, with calcium-green-5N and fluo-3, the dichroic signal reports a net reorientation of indicator molecules away from (rather than toward) the axis of the fiber. It is not known, however, if there is any mechanistic relationship between the dichroic signal of calcium-green-5N and the slow component of this indicator's ΔF signal. ii) In two experiments with calcium-green-5N, ΔF waveforms were measured with four combinations of plane polarized light (0°/0°, 0°/90°, 90°/0°, and 90°/90°; cf. Materials and Methods). In each experiment, within the accuracy of the measurements, all four signals had identical waveforms. Thus, in contrast to results described below with mag-fura-red, there is no evidence that the amplitude of the slow component of calcium-green-5N's ΔF varies with polarized light.

Lower-affinity tricarboxylates with principal absorbance bands at visible wavelengths

Mag-fura-red

Mag-fura-red is a visible-wavelength analogue of furaptra and, like BTC, should in principle be a ratioable indicator. As is apparent in Fig. 1 *D*, the ΔF signal from this indicator is unexpectedly complex. With 480 nm excitation, where a fluorescence decrease is expected in response to a rise in $[Ca^{2+}]$, ΔF is biphasic. At early times, ΔF is indeed negative, with a time of onset that is very close to that expected for $\Delta[Ca^{2+}]$; thus this change probably reflects a rapid binding reaction between Ca^{2+} and mag-fura-red. At later times, however, ΔF rises above baseline, a change not consistent with a simple response to $\Delta[Ca^{2+}]$.

The time course of the slower component of ΔF from mag-fura-red overlaps that expected for the fiber's residual tension response (not recorded in this fiber, but see Fig. 1 *E* for representative tension responses). This component cannot, however, be a movement artifact, because a slower, positive phase of ΔF was a consistent finding in all fibers studied ($N = 7$), even in a fiber stretched to a sarcomere length of 4.5 μm, where fiber movement was completely eliminated. Rather, the slower component of ΔF, like the faster component, must reflect a change in the molecular properties of mag-fura-red. With a λ_{ex} of 480 nm, the average peak amplitude of the slower component divided by that of the faster component was -0.37 ± 0.04 ($N = 7$).

Fig. 4 compares several ΔF and ΔA signals from mag-fura-red measured simultaneously from the same fiber region. In Fig. 4, the upper superimposed pair of traces shows $\Delta F(420)$ and $\Delta F(480)$ (the ΔF signals recorded with $\lambda_{ex}/\lambda_{em}$ = 420/550 and 480/550, respectively). From in vitro measurements (not shown), $\Delta F(420)$ is expected to be insensitive to a change in $[Ca^{2+}]$; thus $\Delta F(420)$ probably provides a direct monitor of the time course of the slow component. Interestingly, the later time courses of the $\Delta F(420)$ and $\Delta F(480)$ signals are essentially identical.

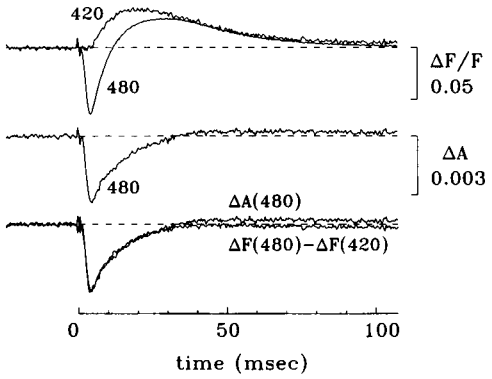

FIGURE 4 ΔF and ΔA signals from a fiber injected with mag-fura-red. The upper pair of traces are $\Delta F/F$ signals recorded with $\lambda_{ex}/\lambda_{em}$ = 420/550 and 480/550, as indicated. The middle trace is $\Delta A(480)$. The lower two traces, which have been scaled to the same peak amplitude, are $\Delta A(480)$ and the difference between the upper pair of fluorescence records (($\Delta F/F$)(480) − ($\Delta F/F$)(420)). Fiber 072993.2

The middle panel of Fig. 4 shows the isotropic absorbance change of mag-fura-red measured at 480 nm, $\Delta A(480)$. Also detected at 480 nm (not shown) was an indicator-related dichroic signal ($\Delta A_0(480) - \Delta A_{90}(480) > 0$). Because the amplitude of this signal was small (+0.00062), the dichroic signal was not analyzed further. In Fig. 4, the rapid time course of the isotropic $\Delta A(480)$ (time to peak, 4.8 ms; half-width, 9.4 ms) is essentially identical to that expected for $\Delta[Ca^{2+}]$. At late times, $\Delta A(480)$ shows a slight positive phase (overshoot of the baseline). The amplitude of this positive phase is a small fraction of the early peak and was not consistently seen in ΔA measurements from all fibers; hence this signal probably represents a small movement artifact. (*Note:* Movement artifacts in the ΔA measurements were generally larger than movement artifacts in the ΔF measurements.)

If calculated from the absorbance measurements (cf. Materials and Methods), the peak value of Δf_{CaD} for mag-fura-red averaged 0.052 ± 0.009 (N = 4). The corresponding peak value of $\Delta[Ca^{2+}]$ is 3.8 μM if calibrated from the in vitro value of $K_{D,\ Ca}$. This value of $\Delta[Ca^{2+}]$ is ~4-fold smaller than the average value estimated with furaptra (cf. column 7 of Table 4), a difference that is likely to be related to the large percentage of mag-fura-red molecules bound to myoplasmic constituents (82%; column 3 of Table 4).

The $\Delta A(480)$ signal indicates, as expected, that the fast decrease in $\Delta F(480)$ is directly linked to a decrease in $\Delta A(480)$ of identical time course. If the slower increase of $\Delta F(480)$ is linked to a slower increase in $\Delta A(480)$, the quantum efficiency of the mechanism relating ΔA and ΔF must be at least an order of magnitude larger for the slower increase than for the fast decrease.

A possible mechanism involved in generation of the slower component of the mag-fura-red signal is an increase in quantum efficiency (with little or no absorbance change) of a subpopulation of dye molecules whose local environment changes in response to fiber activity. An environment change might result from the binding of Ca^{2+} to a receptor protein closely associated with this subpopulation of molecules, i.e., an event similar to that hypothesized to underlie the dichroic signal from the metallochromic dyes (Baylor et al., 1982a) and that may also underlie the mag-fura-red dichroic signal mentioned in the preceding paragraph and the slower ΔF component of the calcium-green-5N signal (see above). From the similarity of the late time course of the $\Delta F(420)$ and $\Delta F(480)$ signals in Fig. 4 (*upper pair of traces*), it appears possible that the amplitude of the slower component of the mag-fura-red signal is independent of $\lambda_{ex}/\lambda_{em}$. If so, a subtraction of the individual signals should eliminate the slower component of ΔF and yield a signal reflective of $\Delta[Ca^{2+}]$. The lower pair of traces in Fig. 4 compares this subtracted signal (($\Delta F/F$)(480) − ($\Delta F/F$)(420)) with mag-fura-red's $\Delta A(480)$ signal. As expected under this hypothesis, the time course of the subtracted signal is essentially identical to that of $\Delta A(480)$ (which, as mentioned above, is close to that expected for $\Delta[Ca^{2+}]$). (*Note:* Under the hypothesis of a change in quantum efficiency, it is not appropriate to use a ratio approach to eliminate the effects of the slow component, because the change in quantum efficiency is hypothesized to apply to a subpopulation of indicator molecules only.)

To further explore the mechanism of mag-fura-red's slower component, the polarization dependence of the signal was examined. As shown by both pairs of superimposed traces in Fig. 5, the amplitude of the slower component was larger when the plane of polarization of the excitation beam was at 0° than at 90°. This difference implies that the slower component probably arises from indicator molecules that have a greater net orientation parallel to, rather than perpendicular to, the axis of the fiber and hence that must, in part, be associated with an oriented structure of myoplasm. In contrast, the fast component of ΔF has the same amplitude in both superimposed pairs in Fig. 5; this result is

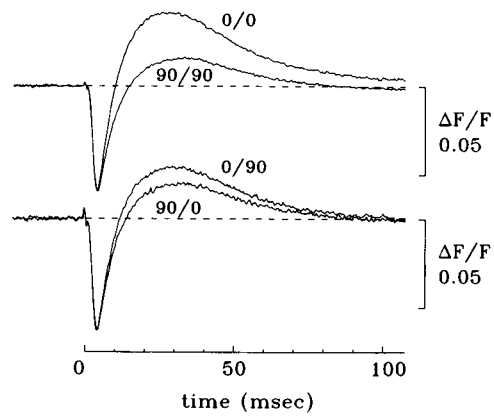

FIGURE 5 ΔF signals ($\lambda_{ex}/\lambda_{em}$ = 480/550 nm) from mag-fura-red measured with plane polarized light. The upper two traces (0/0 and 90/90) were measured with the same plane of polarization for the excitation and emission beams, and the lower two traces (0/90 and 90/0) were measured with the emission beam polarized perpendicular to the excitation beam. Same fiber as Fig. 4.

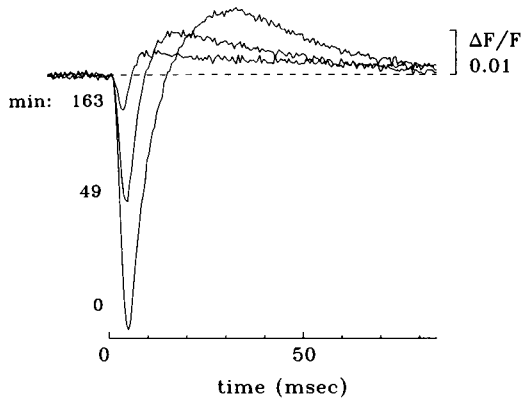

FIGURE 6 ΔF signals ($\lambda_{ex}/\lambda_{em}$ = 480/550) from mag-fura-red measured at different times after exposure of a fiber to BAPTA-AM. The fiber was first loaded with mag-fura-red-AM (loading period of 137 min), then washed with normal Ringer and exposed to BAPTA-AM. The numbers next to the traces indicate time (in minutes) relative to the change to the BAPTA loading solution. Fiber 050594.1.

expected if the fast component directly reflects Ca^{2+} complexation by indicator molecules that are primarily in the myoplasmic solution and thus are unable to react with a polarization preference.

Fig. 6 presents an experiment designed to test whether the amplitude of the slower component of ΔF depends on the amplitude of $\Delta[Ca^{2+}]$. A fiber was first exposed to mag-fura-red by the AM loading technique, which achieved an approximately constant concentration of indicator throughout the fiber; then, later in the experiment, the fiber was exposed to BAPTA-AM. Based on other experiments (Zhao et al., 1995), it was expected that, after exposure to BAPTA-AM for a period of 1–2 h, the myoplasmic concentration of (hydrolyzed) BAPTA would reach ~0.5–1 mM and have a strong buffering effect on $\Delta[Ca^{2+}]$. Indeed, Fig. 6 indicates that the amplitude of $\Delta[Ca^{2+}]$ was greatly reduced by BAPTA, because the amplitude of the fast component of mag-fura-red's ΔF was greatly reduced. Interestingly, the amplitude of the slower component of ΔF was reduced in parallel. This finding implies that the slower component depends rather directly on $\Delta[Ca^{2+}]$ and rules out the possibility that it might reflect the amount or rate of Ca^{2+} release from the sarcoplasmic reticulum (SR). This follows because the amount and peak rate of SR Ca^{2+} release in response to an action potential likely increase in the presence of these concentrations of BAPTA—cf. experiments by Baylor and Hollingworth (1988), Hollingworth et al. (1992), and Pape et al. (1993), which show that fura-2 in myoplasm, at concentrations up to ~4 mM, increases the amount and peak rate of SR Ca^{2+} release. Thus, the slower component of ΔF appears to reflect a change in properties of a subpopulation of mag-fura-red molecules associated, directly or indirectly, with some Ca^{2+}-receptor molecule on an oriented structure in myoplasm.

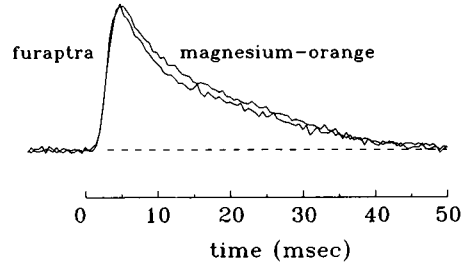

FIGURE 7 Values of ΔF measured simultaneously in the same fiber with furaptra and magnesium orange. The furaptra record is the average of two sweeps taken before and after the magnesium orange signal (two sweeps). The peak amplitudes of $\Delta F/F$ were −0.108 (furaptra) and 0.141 (magnesium orange). See text for values of times to peak and half-widths. Fiber 050495.1; sarcomere length 4.1 μm.

Magnesium orange

Magnesium orange is a tricarboxylate analog of calcium orange; its in vitro $K_{D,\,Ca}$ (43 μM; Table 1) is essentially identical to that of furaptra (44 μM). As shown in Fig. 1, the ΔF from magnesium orange has a waveform that is quite similar to furaptra's. In Table 2, the average values of time to peak and half-width of the ΔF from magnesium orange, 5.0 (± 0.0) ms and 12.5 (± 2.5) ms, are not significantly different from those from furaptra. To compare more precisely the time courses of ΔF from magnesium orange and furaptra, two coinjection experiments of the type illustrated in Fig. 3 were carried out. Fig. 7 shows results from one of these experiments and confirms that the ΔF waveforms from the two indicators are indeed very similar. The time to peak values of ΔF were 5.0 versus 5.0 ms (furaptra versus magnesium orange) and the half-width values were 9.5 versus 11.4 ms. Similar results were seen in the second experiment (not shown), with time to peak values of 4.5 versus 4.5 ms (furaptra versus magnesium orange) and half-width values of 7.2 versus 9.4 ms. Overall, the slightly larger value for the half-width of ΔF from magnesium orange might be explained by one or more of the following possibilities: i) the effective myoplasmic value of k_{-1} of magnesium orange might be slightly limiting—for example, k_{-1} might be 2000–3000 s^{-1}, with the result that the half-width values are detectably larger than those from furaptra; ii) ΔF from magnesium orange might have a small contribution from a slower component of the type inferred for calcium-green-5N (see above); iii) the value of Δf_{CaD} for magnesium orange might be slightly larger than that for furaptra, with the result that its ΔF half-width is slightly larger (this possibility is considered unlikely, however, because of the similarity of the in vitro values of $K_{D,\,Ca}$ for the two indicators and the finding that the bound percentage of magnesium orange, 84%, is greater than that of furaptra, 58%; column 3 of Table 4); iv) in spite of the long sarcomere length of the fibers (4.1 μm and 3.8 μm in the two coinjection experiments), the ΔF signal from one or both indicators might still contain a small movement artifact that makes imprecise an exact comparison of the Ca^{2+}-related

signals (again, this result is considered unlikely, although it cannot be ruled out entirely). Overall, the close similarity in the ΔF time courses from the two indicators supports the idea that the ΔF from magnesium orange tracks $\Delta[Ca^{2+}]$ in a simple and quite rapid fashion.

Magnesium green

Magnesium green is a tricarboxylate version of calcium-green-1; however, its in vitro $K_{D,\,Ca}$ is approximately six-fold smaller than that of magnesium orange and furaptra (Table 1). Thus, Δf_{CaD} would be expected to be larger with magnesium green than with magnesium orange or furaptra, and, if so, the half-width of ΔF with magnesium green should be larger than that observed with the other two indicators. Consistent with this expectation, the average value of magnesium green's half-width (22.6 ± 2.5 ms; Table 2) is significantly larger than that of either magnesium orange (12.5 ± 2.5 ms) or furaptra (10.9 ± 0.7 ms). Additionally, the average value of the time to peak of ΔF from magnesium green, 6.1 ± 0.4 ms, is significantly larger than that observed with either magnesium orange (5.0 ± 0.0 ms) or furaptra (5.0 ± 0.1 ms). As noted earlier with other indicators, a difference in time to peak of this magnitude is consistent with the effective myoplasmic value of k_{-1} of the indictor being slightly rate limiting (k_{-1} of ~1000 s^{-1}).

To compare more accurately the ΔF time courses from magnesium green and furaptra, a single coinjection experiment of the type illustrated in Figs. 3 and 7 was carried out. As is apparent in Fig. 8 *A*, the time to peak and half-width of furaptra's ΔF (5.0 and 13.6 ms, respectively) are indeed briefer than the corresponding values for magnesium green (5.5 and 20.7 ms, respectively).

Fig. 8 *B* compares the time course of $\Delta[Ca^{2+}]$ (calculated from furaptra's ΔF by the method described in connection with Fig. 3 *B*) and the ΔF waveform from magnesium green. The dashed trace in Fig. 8 *B* shows a fit of the type presented in Fig. 3 *B*, which assumes that ΔF from magnesium green reflects a simple kinetic response to $\Delta[Ca^{2+}]$. The good agreement between the measured and the fitted traces demonstrates that magnesium green's response to $\Delta[Ca^{2+}]$ is consistent with myoplasmic values of k_{+1} and k_{-1} of ~9×10^7 M^{-1} s^{-1} and ~1750 s^{-1}, respectively (cf. legend of Fig. 8). As mentioned above in connection with Fig. 3 *B*, the fitted value of k_{+1}, but not k_{-1}, varies directly with the value of Δf_{CaD} assumed for magnesium green, which was 0.5 for the fit of Fig. 8 *B*. The selection of this value was somewhat arbitrary but was based on the value of Δf_{CaD} measured for furaptra in this experiment (0.162) and the observation from the in vitro measurements that $K_{D,\,Ca}$ is substantially smaller for magnesium green than for furaptra.

Unfortunately, because the Ca^{2+}-related absorbance change of magnesium green is significant at UV wavelengths only, it was not possible to make a direct estimate of Δf_{CaD} for magnesium green by ΔA measurements, as was done for BTC and calcium-green-5N. If, however, the value of Δf_{CaD} was substantially smaller than the 0.5 value assumed for the fit of Fig. 8 *B*, the half-width of ΔF from magnesium-green would be larger than could be readily explained by a simple kinetic response to $\Delta[Ca^{2+}]$. Thus, an alternative interpretation, which cannot be ruled out by the experiments, is that the rather large half-width value of ΔF from magnesium green may be due, at least in part, to contamination from a slower component of the type inferred above for calcium-green-5N.

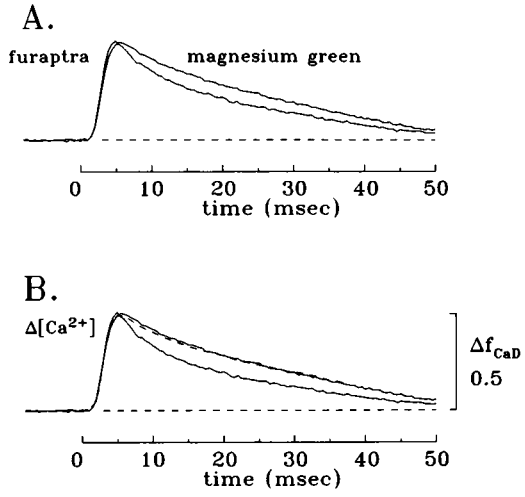

FIGURE 8 (*A*) Values of ΔF measured simultaneously in the same fiber with furaptra and magnesium green. The furaptra record is the average of five sweeps interleaved with the seven sweeps taken for the magnesium green record. See text for values of time to peak and half-width. (*B*) Kinetic fit (*dashed line*) of the magnesium green ΔF signal, carried out by the method described in connection with Fig. 3 *B*. The peak of $\Delta[Ca^{2+}]$ was 19.0 μM. A peak amplitude of 0.5 was assumed for Δf_{CaD} of magnesium green; this is roughly consistent with the 0.162 value of Δf_{CaD} measured for furaptra and the relative values of $K_{D,\,Ca}$ measured for the two indicators in the in vitro calibrations (cf. Table 1). The fitted values of k_{+1} and k_{-1} for magnesium green were 9.3×10^7 M^{-1} s^{-1} and 1764 s^{-1}, respectively. Fiber 062095.2

Amplitude of the maintained component of ΔF from the various indicators

Previous experiments with azo1 (Hollingworth and Baylor, 1986) and fura-2 (Baylor and Hollingworth, 1988) indicate that $\Delta[Ca^{2+}]$ after a single action potential does not return completely to baseline on a fast time scale; rather, $\Delta[Ca^{2+}]$ returns to a maintained (or quasi-steady) level that, by 150–200 ms after stimulation, is about 0.01–0.02 of the peak value of $\Delta[Ca^{2+}]$. Furthermore, previous experiments with furaptra (Konishi et al., 1991) indicate that the final return of this maintained $\Delta[Ca^{2+}]$ to baseline probably takes many seconds, and that associated with the maintained increase in $[Ca^{2+}]$ is a maintained increase in $[Mg^{2+}]$. This $\Delta[Mg^{2+}]$ is thought primarily to reflect an exchange of Ca^{2+} for Mg^{2+} on the metal-binding sites of parvalbumin (see, e.g., Gillis et al., 1982; Baylor et al., 1983) and was first studied experimentally with the absorbance indicator

antipyrylazo III (Baylor et al., 1982b, 1985b; Irving et al., 1989; see also Jacquemond and Schneider, 1992). In the previous experiments with furaptra, the amplitude of ΔF measured 150–200 ms after a single action potential had a quasi-steady level that averaged 0.053 (± 0.004) of the peak value (Konishi et al., 1991). Because this quasi-steady level was about threefold larger than that expected from $\Delta[Ca^{2+}]$ alone (cf. measurements with azo1 and fura-2 mentioned above), it was suggested that ~2/3 of furaptra's maintained ΔF signal is due to $\Delta[Mg^{2+}]$ and ~1/3 to $\Delta[Ca^{2+}]$.

Because the ΔF's from the indicators studied in this article should be sensitive to maintained increases in $[Ca^{2+}]$ and, in some cases, $[Mg^{2+}]$, it was of interest to estimate the quasi-steady levels of ΔF (measured 150–200 ms after stimulation) from the various indicators. This analysis was restricted to lower-affinity indicators only, because, with the higher-affinity indicators, the 150–200-ms time period is not sufficient to guarantee kinetic equilibrium between $\Delta[Ca^{2+}]$ and ΔF. Results with calcium-green-5N and mag-fura-red were also excluded from this analysis because ΔF from these indicators is likely to be contaminated by the slower components discussed above. Fig. 1 illustrates that, during the period 150–200 ms after stimulation, ΔF from most of the remaining indicators was detectably different from baseline. This conclusion is confirmed by the information in column 6 of Table 2, which gives mean values of $\Delta F_{steady}/\Delta F_{peak}$ (the average value of ΔF during the period 150–200 ms after stimulation divided by the peak value of ΔF). For all seven indicators, the mean value of $\Delta F_{steady}/\Delta F_{peak}$ was a positive number (range, 0.015–0.044); these numbers were statistically different from zero for BTC (0.025 ± 0.005), calcium-orange-5N (0.015 ± 0.005), furaptra (0.044 ± 0.005), and magnesium green (0.032 ± 0.004).

With the tetracarboxylate indicators (BTC and calcium-orange-5N), $\Delta F_{steady}/\Delta F_{peak}$ should be insensitive to $\Delta[Mg^{2+}]$. The results with these indicators can therefore be directly converted to an average value of the quasi-steady level of $\Delta[Ca^{2+}]$ divided by the peak of $\Delta[Ca^{2+}]$, 0.012–0.021 (column 7 of Table 2). (*Note:* The latter values are slightly smaller than the average values of $\Delta F_{steady}/\Delta F_{peak}$ because the nonlinearity and slight kinetic lag between $\Delta[Ca^{2+}]$ and ΔF for these indicators act to reduce ΔF_{peak}.) The range 0.012–0.021 for $\Delta[Ca^{2+}]_{steady}/\Delta[Ca^{2+}]_{peak}$ is essentially identical to that inferred previously with azo1 and fura-2 (see above).

Of the tricarboxylate indicators, only furaptra's value of $\Delta F_{steady}/\Delta F_{peak}$ (0.044 ± 0.005) is significantly larger than expected based on information from the tetracarboxylate indicators for $\Delta[Ca^{2+}]_{steady}/\Delta[Ca^{2+}]_{peak}$. As mentioned above, a $\Delta F_{steady}/\Delta F_{peak}$ of larger amplitude than expected for $\Delta[Ca^{2+}]$ alone was previously detected with furaptra and is presumed to reflect $\Delta[Mg^{2+}]$ (Konishi et al., 1991). (*Note:* With the other tricarboxylate indicators, the failure to detect a $\Delta F_{steady}/\Delta F_{peak}$ of amplitude significantly larger than that expected for $\Delta[Ca^{2+}]$ alone may be due to the small number of experiments carried out with these indicators.)

DISCUSSION

This article compares kinetic and other properties of tri- and tetracarboxylate Ca^{2+} indicators microinjected into frog single muscle fibers. As expected, lower-affinity Ca^{2+} indicators, which have larger values of k_{-1}, respond to $\Delta[Ca^{2+}]$ substantially faster than do higher-affinity indicators. Indeed, ΔF signals from three of the five newer tricarboxylate indicators used in this study have time courses essentially identical to that of furaptra (which probably tracks $\Delta[Ca^{2+}]$ without significant delay; Konishi et al., 1991). As argued in the first section of the Results, furaptra's myoplasmic value of k_{-1} is likely to be at least 5000 s^{-1} (at 16°C); thus similar k_{-1} values are likely to apply to mag-fura-5, mag-indo-1, and possibly magnesium orange. With magnesium green, ΔF responds to $\Delta[Ca^{2+}]$ with a detectable delay, corresponding to a k_{-1} of 1000–2000 s^{-1}. This delay appears to be consistent with a myoplasmic k_{-1} of furaptra in excess of 5000 s^{-1} and the lower in vitro value of $K_{D,\,Ca}$ for magnesium green (7 μM compared with furaptra's 44 μM). The ΔF of mag-fura-red, the other tricarboxylate studied, has an early, rapid component (with 480 nm excitation) that appears to track $\Delta[Ca^{2+}]$ without delay (k_{-1} probably $\geq$ 5000 s^{-1}); unfortunately, the time course of this component is obscured by a slower component of ΔF, which greatly limits the usefulness of mag-fura-red for Ca^{2+} measurements in skeletal muscle. Thus, in general, lower-affinity tricarboxylate indicators with in vitro values of $K_{D,\,Ca}$ greater than ~25 μM appear to track $\Delta[Ca^{2+}]$ in skeletal muscle without a detectable delay.

In contrast, ΔF's from the lower-affinity tetracarboxylate indicators (BTC, calcium-orange-5N, and calcium-green-5N) were all slower than that of furaptra. This finding is unexpected, because the in vitro values of $K_{D,\,Ca}$ of these indicators are also $\geq$25 μM. The estimates of k_{-1} for these tetracarboxylate indicators, ~1000 s^{-1}, are severalfold smaller than those estimated for the tricarboxylate indicators; moreover, because of the similar values of $K_{D,\,Ca}$, myoplasmic values of k_{+1} for the tetracarboxylate indicators must also be severalfold smaller. The overall delay due to the reaction rates of BTC, calcium-orange-5N, and calcium-green-5N is not large and is, in principle, easily corrected by computation. However, as discussed in the next section, other, more significant problems were detected with these indicators.

As far as we know, the presence of smaller Ca^{2+} association rates for tetracarboxylate compared with tricarboxylate indicators has not been reported in in vitro measurements, but slower rates might result if the coordination of Ca^{2+} in the tetracarboxylate binding pocket is more structured. Alternatively, the difference in the rates that we estimate for tri- and tetracarboxylate indicators might apply only in the myoplasm and be a consequence of indicator

binding to myoplasmic constituents. For example, indicator binding appears to slow both k_{+1} and k_{-1} (e.g., Baylor et al., 1985a; Baylor and Hollingworth, 1988; Harkins et al., 1993), and the percentage of bound indicator estimated in this study was higher for the lower-affinity tetracarboxylate indicators (89–95%) than for the rapidly reacting tricarboxylates (57–84%).

Another comparison reveals that the reaction rates estimated for the lower-affinity tetracarboxylate indicators, $0.5–1.2 \times 10^7\ M^{-1}\ s^{-1}$ for k_{+1} and $\sim 1000\ s^{-1}$ for k_{-1}, are smaller than might have been expected. Previous experiments at 16°C estimated k_{+1} values of $1.3–2.5 \times 10^7\ M^{-1}\ s^{-1}$ and k_{-1} values of $18–34\ s^{-1}$ for three higher-affinity tetracarboxylate indicators (fura-2, fura-red, and fluo-3; Baylor and Hollingworth, 1988; Hollingworth et al., 1992; Kurebayashi et al., 1993; Harkins et al., 1993). Thus, BTC, calcium-orange-5N, and calcium-green-5N, with in vitro values of $K_{D,\,Ca}$ two orders of magnitude larger than those of the higher-affinity indicators, would be expected to have had similar k_{+1} values but k_{-1} values of $2000–3000\ s^{-1}$. The reason for the two- to threefold smaller observed values is not known but might be a consequence of the somewhat larger percentage of bound indicator estimated for BTC (95%), calcium-orange-5N (89%), and calcium-green-5N (91%) than estimated for fura-2 (76%), fura-red (89%), and fluo-3 (87%) (see Materials and Methods).

Results unique to individual indicators

Of the nine lower-affinity indicators used in this study, three showed clear evidence for the presence of a substantial component of fluorescence not directly related to a simple kinetic reaction with Ca^{2+}. The most unusual result was obtained with mag-fura-red. With 480 nm excitation, ΔF showed a delayed increase after the expected early decrease. Measurements with polarized light indicated that indicator molecules with an absorbance moment oriented parallel to the fiber axis make a greater contribution to this signal than do molecules with a perpendicular absorbance moment. As hypothesized for the dichroic signals from the metallochromic dyes (cf. Baylor et al., 1982a), it is likely that the slow component of the mag-fura-red signal reflects a Ca^{2+}-driven change in a subpopulation of bound and oriented indicator molecules. For example, the slow ΔF from mag-fura-red might report a change in thin filament activation driven by the binding of Ca^{2+} to troponin. Under this hypothesis, it would be of interest in future experiments to characterize more precisely the Ca^{2+} dependence of this signal and perhaps its response to pharmacological agents and its variation among different fiber types.

With calcium-green-5N, the presence of a slow component of ΔF was inferred from a combination of three properties: i) a relatively fast time to peak of ΔF; ii) a relatively small peak value of Δf_{CaD}, yet iii) a broad half-width of ΔF. These features are not consistent with a simple response of ΔF to $\Delta[Ca^{2+}]$. For example, BTC, with a similar time to peak of ΔF and a similar peak value of Δf_{CaD}, had a much smaller value for the half-width of ΔF (16.2 ± 1.0 ms versus 36.7 ± 4.5 ms). Again, the most likely explanation of this slow component is a Ca^{2+}-driven perturbation of a binding reaction between indicator molecules and myoplasmic proteins.

The possibility also exists that the ΔF from calcium-orange-5N could be slightly contaminated by a similar slow component, as the overall time course of the ΔF from calcium-orange-5N was slightly broader than expected from the time course of furaptra's ΔF and a reasonable guess for Δf_{CaD} of calcium-orange-5N (namely, Δf_{CaD} of calcium-orange-5N $\leq \Delta f_{CaD}$ of from furaptra). Unfortunately, because calcium-orange-5N and other related indicators based on a fluorescein chromophore do not have an isosbestic wavelength for fluorescence excitation, a direct measurement of the time course of a possible slow fluorescence component by the method used for mag-fura-red was not possible (cf. the $\Delta F(420)$ trace in Fig. 4). The existence of such a component from calcium-orange-5N, and from other fluorescein-based indicators, remains open.

Additionally, with calcium-orange-5N, a light-dependent reduction in ΔF was observed with 500–550-nm wide-band excitation. A similar effect of illumination was not observed with magnesium orange, and its presence with calcium-orange-5N clearly detracts from the usefulness of this indicator.

Finally, the fluorescence of BTC appears to have a significant sensitivity to some myoplasmic event besides $\Delta[Ca^{2+}]$. This unexpected finding was detected as a drift in the parameter K used in the calculation of BTC's ratio signal (cf. Eqs. 1 and 2). For a well-behaved, lower-affinity indicator, K is expected to be a constant, and the substantial time-dependent change detected with BTC raises serious concerns about the reliability of this indicator for quantitative $[Ca^{2+}]$ measurements. Again, this unexpected feature of BTC is presumed to be related to the very large percentage ($\sim$95%) of this indicator that is bound to myoplasmic constituents.

The general problem of indicator binding to intracellular constituents

As indicated in Tables 3 and 4, a significant percentage of each of the 14 indicators of this study appears to bind to myoplasmic constituents of low mobility (presumed to be proteins), and with 10 of the indicators the bound percentage is estimated to exceed 80%. These findings are in general agreement with the many previous studies in muscle that have reported significant intracellular binding of indicator (see Introduction). Thus, in muscle fibers at least, the existence of a large bound percentage of indicator must be considered the norm. In this and the previous articles, the presence of a large bound percentage has been associated with substantial alterations in the properties of the indicators that relate to the estimation of $[Ca^{2+}]$. For example, as

indicated in column 7 of Table 4, the in vivo values estimated for $K_{D,\,Ca}$ are two- to eightfold larger than the in vitro values given in Table 1. Additionally, the indicators with clearly identified second components (mag-fura-red, calcium-green-5N, BTC) are among the more heavily bound indicators of this study (bound percentages of 82%, 91%, and 95%, respectively). Thus, it is clearly advantageous to have available indicators that are less severely bound.

In this study, the indicators with the smallest bound percentages were those with principal absorbance bands at UV rather than visible wavelengths. For example, with quin-2, mag-fura-5, furaptra, mag-indo-1, and indo-1, bound percentages of 49–81% were estimated (Tables 3 and 4). Thus, the chemical changes required to produce a longer-wavelength indicator appear to increase the likelihood of binding. (An exception to this rule is provided by PDAA, which has the smallest bound percentage of any indicator studied in intact muscle fibers; the chemical structure of purpurate-based compounds, however, is quite different from that of the tri- and tetracarboxylate indicators.)

A suggestion for a better lower-affinity Ca^{2+} indicator

A disappointing outcome of the present experiments was that only the shorter wavelength, lower-affinity indicators (mag-fura-5 and mag-indo-1) equaled furaptra in the combined attributes of a rapid kinetic response to Ca^{2+} and a $\Delta F/F$ signal that is readily calibrated in units of Δf_{CaD}. Moreover, the bound percentages of all the visible wavelength indicators exceeded those of furaptra, mag-fura-5, and mag-indo-1. Table 1 suggests that, in comparison with furaptra, mag-indo-1 has the advantage of a somewhat higher affinity for Ca^{2+} and a greater selectivity for Ca^{2+} over Mg^{2+}. The experimental results, however, showed no significant difference between mag-indo-1 and furaptra in either the amplitude of Δf_{CaD}, a quantity that should vary inversely with the intracellular value of $K_{D,\,Ca}$, or in the value of $\Delta F_{steady}/\Delta F_{peak}$, a quantity that should vary directly with the intracellular $K_{D,\,Ca}$ divided by the intracellular $K_{D,\,Mg}$. Whether significant differences between furaptra and mag-indo-1 would be found with a larger experimental sample remains an open question.

Because the ΔF signal from a tetracarboxylate Ca^{2+} indicator should be insensitive to $[Mg^{2+}]$, it would clearly be advantageous to have lower-affinity tetracarboxylate indicators other than calcium-orange-5N and calcium-green-5N. (As noted above, significant problems were detected with both of these tetracarboxylate indicators.) We suggest that the "5N" versions of indo-1, quin-2, fura-2, and perhaps fura-red would be valuable additions to the set of lower-affinity Ca^{2+} indicators. Indicators based on these chromophores have the advantage of being ratioable, and their $\Delta F/F$ measurements can be readily scaled to units of Δf_{CaD}. Additionally, because indo-1, quin-2, and fura-2 are shorter wavelength indicators, it is expected that the percentages of indo-1–5N, quin-2–5N, and fura-2–5N that bind to intracellular constituents will be substantially less than observed in this study for calcium-orange-5N and calcium-green-5N. Thus, it is also possible that indo-1–5N, quin-2–5N, and fura-2–5N will respond to $[Ca^{2+}]$ without a detectable delay.

APPENDIX

A derivation is given for Eq. 1 that permits calculation of a ratio signal that is linear in Δf_{CaD} (the change in the fraction of the indicator in the Ca^{2+}-bound form). The approach is based on that of Grynkiewicz et al. (1985) and assumes that fluorescence arises from two forms of the indicator, Ca^{2+}-free and Ca^{2+}-bound, and that fluorescence measurements have been made with two wavelength pairs (denoted 1 and 2). Equations 1a and 1b of Grynkiewicz et al. (1985), applied to the resting fluorescence measured at the two wavelengths, give

$$F_1 = S_{f1}\,c_f + S_{b1}\,c_b \tag{A1}$$

$$F_2 = S_{f2}\,c_f + S_{b2}\,c_b\,, \tag{A2}$$

where c_f and c_b refer to the resting concentrations of Ca^{2+}-free and Ca^{2+}-bound indicators, respectively. S_{f1} and S_{b1} give the proportionality factors between concentration and fluorescence for Ca^{2+}-free and Ca^{2+}-bound indicator at wavelength pair 1; S_{f2} and S_{b2} give analogous factors at wavelength pair 2. These factors depend on the indicator and the recording system.

Let Δ refer to a change with respect to the resting condition and $'$ to a change that arises from $\Delta[Ca^{2+}]$ only. Then, for an indicator with 1:1 stoichiometry (for which $\Delta c_f' = -\Delta c_b'$),

$$\Delta F_1' = (S_{b1} - S_{f1})\,\Delta c_b' \tag{A3}$$

$$\Delta F_2' = (S_{b2} - S_{f2})\,\Delta c_b'\,. \tag{A4}$$

The ratio $\Delta F_1'/\Delta F_2'$ of these fluorescence changes is a constant, k, given by

$$k = (S_{b1} - S_{f1})/(S_{b2} - S_{f2})\,. \tag{A5}$$

If k is normalized by the ratio of the resting fluorescences, another constant, K, is obtained:

$$K = (\Delta F_1'/F_1)/(\Delta F_2'/F_2)\,. \tag{A6}$$

In general, F_1/F_2 depends on c_f/c_b (or, alternatively, f_{CaD}, the resting fraction of the indicator in the Ca^{2+}-bound form). Thus, with a higher-affinity indicator, K might vary during the course of an experiment, if resting $[Ca^{2+}]$ should change.

The ratio approach corrects for any non-Ca^{2+}-related effect on fluorescence that is fractionally the same for Ca^{2+}-free and Ca^{2+}-bound indicator and for the two wavelength pairs, e.g., as might arise from a fractional change in the number of indicator molecules within the optical recording field (denoted $\Delta N/N$). Let ΔF denote the fluorescence change that arises from both $\Delta[Ca^{2+}]$ and $\Delta N/N$. According to the assumptions

$$F_1 + \Delta F_1 = (F_1 + \Delta F_1')\,(1 + \Delta N/N) \tag{A7}$$

$$F_2 + \Delta F_2 = (F_2 + \Delta F_2')\,(1 + \Delta N/N)\,. \tag{A8}$$

Equations A6, A7, and A8 can be rearranged to give Eqs. 1 and 2:

$$\Delta F_1'/F_1 = \frac{-K\,(\Delta F_1/F_1 - \Delta F_2/F_2)}{(1 - K + \Delta F_1/F_1 - K\,\Delta F_2/F_2)} \tag{A9}$$

and

$$\Delta N/N = \frac{(\Delta F_1/F_1 - K\,\Delta F_2/F_2)}{(1 - K)}. \qquad \text{(A10)}$$

Use of Eqs. A9 and A10 requires that K not be equal to 1. Thus, fluorescence can be sensitive to Ca^{2+} at both wavelengths, but not equally so.

In the Results, Eqs. A9 and A10 are applied to a $\Delta N/N$ occurring on a fast time scale due to a movement artifact, but slower changes are also amenable to correction, e.g., as might arise from diffusion of indicator molecules into or out of the optical recording field. As noted by Grynkiewicz et al. (1985), the same equations used to correct for changes in dye content may also apply to some effects that arise from changes in instrumental sensitivity—for example, a wavelength-independent change in lamp intensity.

We thank Mr. Joseph Pili of the Physiology Department machine shop for help with the design and construction of equipment. Drs. Knox Chandler and Masato Konishi provided helpful comments on the manuscript.

This work was supported by grants to SMB from the U.S. National Institutes of Health (NS 17620) and the Muscular Dystrophy Association.

REFERENCES

Baker, A. J., R. Brandes, J. H. M. Schreur, S. A. Camacho, and M. W. Wiener. 1994. Protein, and acidosis alter calcium-binding, and fluorescence spectra of the calcium indicator indo-1. *Biophys. J.* 67: 1646–1654.

Bassani, J. W. M., R. A. Bassani, and D. M. Bers. 1995. Calibration of indo-1 and resting intracellular $[Ca]_i$ in intact rabbit cardiac myocytes. *Biophys. J.* 68:1453–1460.

Baylor, S. M., W. K. Chandler, and M. W. Marshall. 1982a. Dichroic components of arsenazo III and dichlorophosphonazo III signals in skeletal muscle fibres. *J. Physiol.* 331:179–210.

Baylor, S. M., W. K. Chandler, and M. W. Marshall. 1982b. Use of metallochromic dyes to measure changes in myoplasmic calcium during activity in frog skeletal muscle fibres. *J. Physiol.* 331:139–177.

Baylor, S. M., W. K. Chandler, and M. W. Marshall. 1983. Sarcoplasmic reticulum calcium release in frog skeletal muscle fibres estimated with arsenazo III calcium transients. *J. Physiol.* 344:625–666.

Baylor, S. M., and S. Hollingworth. 1988. Fura-2 calcium transients in frog skeletal muscle fibres. *J. Physiol.* 403:151–192.

Baylor, S. M., and S. Hollingworth. 1991. Absorbance signals from resting frog skeletal muscle fibers injected with the pH indicator dye, phenol red. *J. Gen. Physiol.* 96:449–471.

Baylor, S. M., S. Hollingworth, C. S. Hui, and M. E. Quinta-Ferreira. 1985a. Calcium transients from intact frog skeletal muscle fibres simultaneously injected with antipyrylazo III, and Azo1. *J. Physiol.* 365:70P.

Baylor, S. M., S. Hollingworth, C. S. Hui, and M. E. Quinta-Ferreira. 1986. Properties of the metallochromic dyes arsenazo III, antipyrylazo III, and azo1 in frog skeletal muscle fibres at rest. *J. Physiol.* 377:89–141.

Baylor, S. M., S. Hollingworth, and M. Konishi. 1989. Calcium transients in intact frog single skeletal muscle fibres measured with the fluorescence indicator dye Mag-fura-2. *J. Physiol.* 418:69P.

Baylor, S. M., and H. Oetliker. 1977. A large birefringence signal preceding contraction in single twitch fibers of the frog. *J. Physiol.* 264: 141–162.

Baylor, S., M. E. Quinta-Ferreira, and C. S. Hui. 1985b. Isotropic components of antipyrylazo III signals from frog skeletal muscle fibers. *In* Calcium and Biological Systems. R. P. Rubin, G. Weiss, and J. W. Putney, Jr., editors. Plenum Publishing, New York. 339–349.

Beeler, T. J., A. Schibeci, and A. Martonosi. 1980. The binding of arsenazo III to cell components. *Biochim. Biophys. Acta.* 629:317–327.

Blinks, J. R., R. Rudel, and S. R. Taylor. 1978. Calcium transients in isolated amphibian skeletal muscle fibres: detection with aequorin. *J. Physiol.* 277:291–323.

Cifuentes, F., A. L. Escobar, and J. Vergara. 1993. Calcium-orange-5N: a low affinity indicator able to track the fast release of calcium in skeletal muscle fibers. *Biophys. J.* 68:A419.

Claflin, D. R., D. L. Morgan, D. G. Stephenson, and F. J. Julian. 1994. The intracellular Ca^{2+} transient and tension in frog skeletal muscle fibres measured with high temporal resolution. *J. Physiol.* 475:319–325.

DeMarinis, R. M., H. E. Katerinopoulos, and K. A. Muirhead. 1990. New tetracarboxylate compounds as fluorescent intracellular calcium indicators. *Biochem. Methods.* 112:381.

Gillis, J. M., D. Thomason, J. Lefevre, and R. H. Kretsinger. 1982. Parvalbumins and muscle relaxation: a computer simulation study. *J. Muscle Res. Cell Motil.* 3:377–398.

Grynkiewicz, G., M. Poenie, and R. Y. Tsien. 1985. A new generation of Ca^{2+} indicators with greatly improved fluorescence properties. *J. Biol. Chem.* 260:3440–3450.

Harkins, A. B., N. Kurebayashi, and S. M. Baylor. 1993. Resting myoplasmic free calcium in frog skeletal muscle fibers estimated with fluo-3. *Biophys. J.* 65:865–881.

Haugland, R. P. 1992. Handbook of Fluorescent Probes and Research Chemicals, 5th Ed. Molecular Probes, Eugene, OR.

Hirota, A., W. K. Chandler, P. L. Southwick, and A. S. Waggoner. 1989. Calcium signals recorded from two new purpurate indicators inside frog cut twitch fibers. *J. Gen. Physiol.* 94:597–631.

Hollingworth, S., and S. M. Baylor. 1986. Calcium transients in frog skeletal muscle fibers injected with Azo1, a tetra-carboxylate Ca^{2+} indicator. *In* Optical Methods in Cell Physiology. P. De Weer and B. M. Salzberg, editors. John Wiley and Sons, New York. 261–283.

Hollingworth, S., A. B. Harkins, N. Kurebayashi, M. Konishi, and S. M. Baylor. 1992. Excitation-contraction coupling in intact frog skeletal muscle fibers injected with mmolar concentrations of fura-2. *Biophys. J.* 63:224–234.

Hove-Madsen, L., and D. M. Bers. 1992. Indo-1 binding to protein in permeabilized ventricular myocytes alters its spectral and Ca binding properties. *Biophys. J.* 63:89–97.

Huxley, A. F., and L. D. Peachey. 1961. The maximum length for contraction in vertebrate striated muscle. *J. Physiol.* 156:150–165.

Iatridou, H., E. Foukaraki, M. A. Kuhn, E. M. Marcus, R. P. Haugland, and H. E. Katerinopoulos. 1994. The development of a new family of intracellular calcium probes. *Cell Calcium.* 15:190–198.

Irving, M., J. Maylie, N. L. Sizto, and W. K. Chandler. 1989. Simultaneous monitoring of changes in magnesium and calcium concentrations in frog cut twitch fibers containing antipyrylazo III. *J. Gen. Physiol.* 93: 585–608.

Jacquemond, J., and M. F. Schneider. 1992. Effects of low myoplasmic Mg^{2+} on calcium binding by parvalbumin and calcium uptake by the sarcoplasmic reticulum in frog skeletal muscle. *J. Gen. Physiol.* 100: 115–135.

Kao, J. P. Y., and R. Y. Tsien. 1988. Ca^{2+} binding kinetics of fura-2 and azo-1 from temperature-jump relaxation measurements. *Biophys. J.* 53: 635–639.

Klein, M. G., B. J. Simon, G. Szucs, and M. F. Schneider. 1988. Simultaneous recording of calcium transients in skeletal muscle using high and low affinity calcium indicators. *Biophys. J.* 53:971–988.

Konishi, M., and S. M. Baylor. 1991. Myoplasmic calcium transients monitored with purpurate indicator dyes injected in intact frog skeletal muscle fibers. *J. Gen. Physiol.* 97:245–270.

Konishi, M., S. Hollingworth, A. B. Harkins, and S. M. Baylor. 1991. Myoplasmic calcium transients in intact frog skeletal muscle fibers monitored with the fluorescent indicator furaptra. *J. Gen. Physiol.* 97: 271–301.

Konishi, M., A. Olson, S. Hollingworth, and S. M. Baylor. 1988. Myoplasmic binding of fura-2 investigated by steady-state fluorescence and absorbance measurements. *Biophys. J.* 54:1089–1104.

Konishi, M., N. Suda, and S. Kurihara. 1993. fluorescence signals from the Mg^{2+}/Ca^{2+} indicator furaptra in frog skeletal muscle fibers. *Biophys. J.* 64:223–239.

Kurebayashi, N., A. B. Harkins, and S. M. Baylor. 1993. Use of fura red as an intracellular calcium indicator in frog skeletal muscle fibers. *Biophys. J.* 64:1934–1960.

Kushmerick, M. J., and R. J. Podolsky. 1969. Ionic mobility in muscle cells. *Science.* 166:1297–1298.

Lattanzio, F. A., and D. K. Bartschat. 1991. The effect of pH on rate constants, ion selectivity and thermodynamic properties of fluorescent calcium and magnesium indicators. *Biochem. Biophys. Res. Commun.* 177:184–191.

Maylie, J., M. Irving, N. L. Sizto, G. Boyarsky, and W. K. Chandler. 1987a. Calcium signals recorded from cut frog twitch fibers containing tetramethyl-murexide. *J. Gen. Physiol.* 89:145–176.

Maylie, J., M. Irving, N. L. Sizto, and W. K. Chandler. 1987b. Calcium signals recorded from cut frog twitch fibers containing antipyrylazo III. *J. Gen. Physiol.* 89:83–143.

Maylie, J., M. Irving, N. L. Sizto, and W. K. Chandler. 1987c. Comparison of arsenazo III signals optical signals in intact, and cut frog twitch fibers. *J. Gen. Physiol.* 89:41–81.

Minta, A., J. P. Y. Kao, and R. Y. Tsien. 1989. Fluorescent indicators for cytosolic calcium based on rhodamine and fluorescein chromophores. *J. Biol. Chem.* 264:8171–8178.

Pape, P. C., D.-S. Jong, W. K. Chandler, and S. M. Baylor. 1993. Effect of fura-2 on action potential-stimulated calcium release in cut twitch fibers from frog muscle. *J. Gen. Physiol.* 102:295–332.

Raju, B., E. Murphy, L. A. Levy, R. D. Hall, and R. E. London. 1990. A fluorescent indicator for measuring cytosolic free magnesium. *Am. J. Physiol.* 256:C540–C548.

Tsien, R. Y. 1980. New calcium indicators and buffers with high selectivity against magnesium and protons: design, synthesis, and properties of prototype structures. *Biochemistry.* 19:2396–2404.

Uto, A., H. Arai, and Y. Ogawa. 1991. Reassessment of fura-2 and the ratio method for determination of intracellular Ca^{2+} concentrations. *Cell Calcium.* 12:29–37.

Vergara, J., and A. Escobar. 1993. Detection of Ca^{2+} transients in skeletal muscle fibers using the low affinity dye calcium-green-5N. *Biophys. J.* 64:A37.

Zhao, M., S. Hollingworth, and S. M. Baylor. 1995. AM loading of calcium indicators into frog skeletal muscle fibers. *Biophys. J.* 68:A418.